

AD-A063 764

ARMY MATERIALS AND MECHANICS RESEARCH CENTER WATERTO--ETC F/6 20/11
SMALL-SCALE YIELDING CALCULATION OF TRANSITION TEMPERATURE AND --ETC (U)
AUG 78 R BEEWKES

UNCLASSIFIED

AMMRC-TR-78-36

NL

|OF|
AD
A083784



END
DATE
FILMED
3-79
DDC

AD A063764

AMMRC TR 78-36

LEVEL II

AD

12
NW

SMALL-SCALE YIELDING CALCULATION OF TRANSITION TEMPERATURE AND TOUGHNESS

DDC FILE COPY.

August 1978

Approved for public release; distribution unlimited.

ARMY MATERIALS AND MECHANICS RESEARCH CENTER
Watertown, Massachusetts 02172

DDC
RECEIVED
JAN 26 1979
REGULATED
D

79 01 22 039

The findings in this report are not to be construed as an official Department of the Army position, unless so designated by other authorized documents.

Mention of any trade names or manufacturers in this report shall not be construed as advertising nor as an official indorsement or approval of such products or companies by the United States Government.

DISPOSITION INSTRUCTIONS

Destroy this report when it is no longer needed.
Do not return it to the originator.

UNCLASSIFIED

SECURITY CLASSIFICATION OF THIS PAGE (When Data Entered)

REPORT DOCUMENTATION PAGE

READ INSTRUCTIONS BEFORE COMPLETING FORM

1. REPORT NUMBER 14 AMMRC-TR-78-36		2. GOVT ACCESSION NO.	3. RECIPIENT'S CATALOG NUMBER
4. TITLE (and Subtitle) 6 SMALL-SCALE YIELDING CALCULATION OF TRANSITION TEMPERATURE AND TOUGHNESS		5. TYPE OF REPORT & PERIOD COVERED 9 Final Report	
7. AUTHOR(s) 10 REINIER BEEUWKES, Jr.		8. CONTRACT OR GRANT NUMBER(s)	
9. PERFORMING ORGANIZATION NAME AND ADDRESS Army Materials and Mechanics Research Center Watertown, Massachusetts 02172 DRXMR- TM		10. PROGRAM ELEMENT, PROJECT, TASK AREA & WORK UNIT NUMBERS 16 D/A Project LL161102AH42 AMCMS Code: 611102.H420011	
11. CONTROLLING OFFICE NAME AND ADDRESS U. S. Army Materiel Development and Readiness Command, Alexandria, Virginia 22333		12. REPORT DATE 11 August 1978	
14. MONITORING AGENCY NAME & ADDRESS (if different from Controlling Office) 12 42p.		13. NUMBER OF PAGES 36	
		15. SECURITY CLASS. (of this report) Unclassified	
16. DISTRIBUTION STATEMENT (of this Report) Approved for public release; distribution unlimited.		15a. DECLASSIFICATION/DOWNGRADING SCHEDULE	
17. DISTRIBUTION STATEMENT (of the abstract entered in Block 20, if different from Report)			
18. SUPPLEMENTARY NOTES			
19. KEY WORDS (Continue on reverse side if necessary and identify by block number) Fracture toughness Case studies Transition temperature Mechanical properties Failure (materials) Crack-tip stresses			
20. ABSTRACT (Continue on reverse side if necessary and identify by block number) (SEE REVERSE SIDE)			

UNCLASSIFIED

SECURITY CLASSIFICATION OF THIS PAGE(When Data Entered)

Block No. 20

ABSTRACT

K SUB IC

Toughness and a toughness transition temperature for a crack-like notch are calculated for small-scale yielding corresponding to K_{Ic} test conditions using a macroscopic material failure representation. This transition is the point about which the failure position changes from the notch tip to a subsurface position or vice versa. In lieu of an exact solution for stresses, three cases are treated to provide reasonable bounds. Case II appears to be quantitatively exact at sufficient distances from the crack tip.

- Case I. Stresses are from usual elasticity theory.
- Case II. Stresses are from usual elasticity theory, but strains are from a two-straight-line stress-strain relationship and deformations and boundary movement may be large.
- Case III. Strains are from usual elasticity theory on the argument that even in the yielded region they are substantially contained within a fairly rigid elastic mass.

The transition is found to be independent of the tip radius. Because of its simplicity and consequent clarity, Case I is most extensively discussed. However, if the work-hardening rate of the notch material is very low, Case II must be employed.

LEVEL II

APPROVED BY	
OTD	With Section <input checked="" type="checkbox"/>
DDC	Self Section <input type="checkbox"/>
UNANNOUNCED	<input type="checkbox"/>
JUSTIFICATION	
BY	
DISTRIBUTION/AVAILABILITY CODES	
Dist.	AVAIL. and/or SPECIAL
A	

DDC
RECEIVED
JAN 26 1979
D

UNCLASSIFIED

SECURITY CLASSIFICATION OF THIS PAGE(When Data Entered)

CONTENTS

	Page
NOTATION	v
ABSTRACT	
INTRODUCTION	1
PART I. TRANSITION TEMPERATURE AND ASSOCIATED PROPERTIES SIMPLY BASED ON NOTCH ELASTIC STRESS	
Normal and Shearing Stresses Along Crack Axis	3
Fracture and Transition Temperature	
1. Fracture in General	5
2. Notch Formulae	7
3. Transition Yield Strength and Temperature	7
Toughness	8
Note on Tip Radius	11
PART II. TRANSITION PROPERTIES CONFORMING TO A TWO-SEGMENT STRESS-STRAIN CURVE AND ASSOCIATED FINITE BOUNDARY DISPLACEMENTS	13
Strains in Parabolic Coordinate	13
Near Tip Elastic Stresses in Parabolic Coordinates	14
Strain for Plane Strain with a Piecewise Linear Stress-Strain Relation	14
Strain and Axial Displacement U in Parabolic Coordinates on $v = 0$ Axis, for $\nu = \beta = 1/2$ for a Piecewise Linear Stress-Strain Relation	16
INCREMENTAL THEORY	
Relation between Instantaneous and Initial Values of u for $v = 0$	18
Stresses	19
Transition	23
Transition: Approximation	25
Loading Stress and Toughness at the Transition	26
PART III. TRANSITION PROPERTIES BASED ON NOTION OF ELASTICALLY LIMITED STRAIN AND A SLIP LINE THEORY	27
Contained Strain Theory and Comparison with the Contained Stress Theories	27
APPENDIX A. NEAR TIP STRESSES ALONG A CRACK-LIKE NOTCH AXIS IN TERMS OF POLAR, RECTANGULAR, AND PARABOLIC COORDINATES FOR A LOADING STRESS ACTING PERPENDICULARLY TO THE NOTCH AXIS	31
Polar and Rectangular Coordinates	31
Parabolic Coordinates	31

NOTATION
(In approximate order of occurrence)

K_{Ic}	Critical Stress Intensity
K	Stress Intensity
σ, S	Stress (S_r , Radially, S_θ Perpendicularly to Radius)
k, k_I	Stress Concentration Coefficient
$p (=S_I)$	Loading Stress (Acting Perpendicularly to Notch Axis)
a	Notch Depth
ρ	Tip Radius of Coordinate $u = \sqrt{\rho/a}$
ρ_{00}	Notch Tip Radius Corresponding to $u = u_{00} = \sqrt{\rho_{00}/a}$
r, θ	r = Radial Coordinate, θ = Angular Coordinate (from Crack Axis, Extended)
x, y	Rectangular Coordinates
u, v	Parabolic Coordinates ($u = u_{00} =$ Notch Coordinate)
Y	Tensile Yield Strength
S_s	Shear Stress
u_{00}	Initial Value of u at Notch Tip, an Effective Value of $\sqrt{\rho/a}$
u_0	Value of u at Notch Tip when Loading Stress is p (Incremental Theory)
u_Y	Value of u at Yield Boundary
L_{00}	Yu_{00}/p
F	Fracture Stress
F_Y	Nil-Ductility Fracture Stress (Occurs at $S = Y$, Closely)
F_D	Fracture Stress at Ductility Limit
F_{DC}	Fracture Stress at Ductility Limit when $Y = F_D$ (Closely)
e	Strain
e_D	Strain at Ductility Limit
R.A.	Reduction of Area
S_0	A Constant in the Arc Sinh Stress-Strain Relationship
Y_0, C	Constants in the Yield Strength-Temperature Relationship
T	Absolute Temperature ($^{\circ}K \equiv$ Degrees Kelvin, $^{\circ}F \equiv$ Degrees Fahrenheit)
T_T	Transition Temperature
$F_{DO} e_{DO}$	Known Corresponding Values of F_D and e_D on the F_D Versus e_D Relationship
H	Hardness
E	Young's Modulus of Elasticity
E_t	E_{tan} Secant Modulus (Measured from Y)
$h_u^2 = h_v^2 =$	$u^2 + v^2$
U, V	Displacements of u, v Perpendicular to u and v , Respectively
e_u, e_v	Strains in the Directions Perpendicular to u and v Contours, Respectively
γ_{uv}	Shear Strain Corresponding to u, v Coordinates

σ_u, σ_v	Stresses Corresponding to e_u, e_v
σ_{uv}	Stress Corresponding to γ_{uv}
σ_e	Equivalent Tensile Stress
σ_{kk}	Sum of Principal Stresses
S_{ij}, e_{ij}	Stresses and Strains in General
Σ	Notation for Summation
δ_{ij}	Kronecker Delta
ν	Poisson's Ratio
λ	A Constant (see Text)
$\alpha =$	$1 - Y/\sigma_e$
$\beta =$	$(\nu + \lambda \alpha/3)/(1 + 2\lambda \alpha/3)$
e_{11}, e_{22}	Principal Normal Strain in Plane Strain Hooke's Law
$\sigma_{11}, \sigma_{22}, \sigma_{33}$	Principal Normal Stresses in Plane Strain Hooke's Law
$M =$	$(3/2 + \lambda)/E$
p_Y	Loading Stress at Yield Point at Tip of Notch
U_Y	U when $p = p_Y$
$x =$	u_0/u (Incremental Theory)
$u_i =$	Initial Value of u (Incremental Theory)
$u_0 =$	Notch Tip u Corresponding to Loading Stress p; $u_0 = u_{00}$ Initially
u_{0Y}	u_0 for $p = p_Y$
$\bar{S} =$	$\sigma_v + \sigma_u$ (Incremental Theory)
$\bar{D} =$	$\sigma_v - \sigma_u$ (Incremental Theory)
$R =$	u_0/u_{0y}
$\bar{Y} =$	$2Y/\sqrt{3}$
$\bar{E} =$	$E/(1 - \nu^2)$
$\angle =$	Change in Direction of Shear Stress Trajectory
$\bar{E}_s =$	F_D/e_D
$L =$	$(\bar{Y}/p)/\sqrt{\rho/a}$

INTRODUCTION

Design and material selection against complete brittle failure is based on toughness or transition temperature apart from redundancy of load supporting elements and crack stoppers. Through experimentally determined K_{Ic} values many designers now hope to eliminate failure by the association of failure loads with flaw sizes. However, metallurgical and mechanical engineers have for many years eliminated catastrophic failure by using materials whose transition temperature was below the operating temperature, having observed that with such materials there is no catastrophic fragmentation or abrupt crack growth even though deep cracks were present. Strong materials of this type are classed as tough.

This paper is written to show how a transition temperature and toughness may be calculated assuming that a macroscopic fracture theory (the bounding envelope of stress-strain curves), and the elastic formulae for stresses or for strains near a notch tip with a small radius, are as applicable as they are for K_{Ic} use.

For our calculation the macroscopic theory must not only contain a dependence on temperature or strain-rate as stress-strain curves do, but must contain a higher fracture stress for ductile than for brittle, so-called nil-ductility, fracture.

In regard to the assumption of a crack tip radius, some assumption is necessary to our analysis that permits quantitative comparison of subsurface and notch tip stress. A tip radius does this and seems to be plausible and the simplest. Work hardening, at least as treated here, does not seem to be sufficient in itself. However, in retrospect, it may be noted that in place of the assumption of a tip radius, there could be substituted the assumption that the stresses at the tip are those of the macroscopic tensile stress-strain curve, increasing under load as they would if there were a radius, so that the tip radius presently contained in a parameter of the theory may or may not be considered to be an actual radius. The tip radius does not appear in the final expression for transition temperature.

With respect to our assumption of applicability of the elastic stress or strain formulae to our case of small-scale yielding, we consider notch behavior for two widely different cases which should together embrace actuality. One is that the strains in the yielded region are essentially the same as the elastic strains, since they are contained within a relatively vast elastic region. The other is that the stresses are the same as the elastic stresses. Thus, the strains may be large at the tip of the notch, corresponding to these stresses and the shape of the stress-strain curve.

The first case, confined strain, i.e., strains from elastic theory, has already been utilized¹ to give fracture stresses and tip radii from experimental K_{Ic} tests (made, as necessary, under K_{Ic} conditions). In this case use is made of a theoretical curve which, as we show here, may be interpreted to be an expression showing the relationship between ductility or ductile fracture stress, nil-ductility fracture stress, and yield strength at the transition. This treatment of our problem is contained in Part III of this paper. It could be used along the lines of this paper (if as is here done, the fracture stress condition and tip radii were assumed known) to compute toughness as well as transition temperature.

The second approach, stresses from elastic theory, is not only interesting for comparison with the confined strain case, but because there is indication² that for certain types of stress-strain curves the dominant term in the actual, very complicated stress function for cracks is the ordinary Airy stress function. That is, as approach to the crack tip is considered, the Airy function is quantitatively dominant. This is evidently the case also for very narrow deep notches and, of course, the elastic solution always does hold for large distances from the crack tip.

1. BEEUWKES, R. Jr. *Characteristics of Crack Failure*. Surface and Interfaces, v. II, 1968, p. 277.

2. HUTCHINSON, J. W. *Singular Behavior at the End of a Tensile Crack in a Hardening Material*. J. Mech. Phys. Solids, v. 16, 1968, p. 13-31.

This approach is utilized in Parts I and II. In Part I, boundary movement is assumed to be negligible (as in usual elasticity treatments) and the formulae and analyses are simple and easy to follow. Thus, this case has been treated rather fully.

In Part II, boundary change produced by loading is included in the analysis. It is shown that this change may substantially modify the results of Part I in the case of rather flat hardening slope stress-strain curves associated with high yield strength.

Quantitatively the two approaches do not necessarily lead to substantially different results. In each case in the transition relationship the stress (or strain) at the notch tip is the tensile fracture stress (or ductility), and the stress at or near the elastic-plastic boundary is the nil-ductility fracture stress, while for many stress-strain curves the only other variable having an appreciable effect appears to be the yield strength. If the yield regions and the shear stress trajectories in the yield region are essentially like the elastic ones, then the nil-ductility fracture stress should also be comparable in the two cases.

The transition spoken of here corresponds to a change in fracture location as temperature (or yield strength) is altered. Thus, as testing temperature is lowered, separation of material may change from occurrence at the crack (considered as a notch) tip to a subsurface separation. The latter may be expected to be less sensitive to load maintenance or rate of application than the former for it corresponds to a jumping ahead of the fracture and may thus correspond to an almost immediate cataclysmic failure.

We emphasize that the transition treated is for small-scale yielding as it occurs in K_{Ic} testing. The equations used do not hold if the material yields extensively, even if through-the-section yielding does not occur. Thus, they do not hold if the difference in the loading stress perpendicular to and along the crack axis is close to the yield strength of the material employed.

However, although the appropriate application of our result may be characterized by the conditions of K_{Ic} testing, it is desirable to point out and briefly discuss other transitions than the one treated here, especially since some (e.g., those associated with the Charpy or keyhole test) have been used for applications where the failure behavior seems quite different from that associated with the test (e.g., Charpy or Keyhole) itself. Our small-scale yielding transition, as well as the transition from temperature-insensitive to temperature-sensitive values of K , may be far less severe for some K_{Ic} type specimens than the transition observed with Charpy specimens, i.e., the transition temperature may be much lower for the K_{Ic} specimens than for the Charpy specimens.

In particular, we may plausibly define a partial-to-through-yielding transition, for it is evident that separation with through-section yielding may progress with great energy absorption as in bending a Charpy specimen into two pieces at sufficiently high temperature, while it is difficult to see how such energy absorption could occur if yielding were only partial.

It appears* from experimental observation (in the useful Charpy test range of conditions) that the breakdown in Charpy energy absorption occurs in the fully plastic range. That is, much bending with wide notch opening and deepening with a fibrous fracture appearance occurs down to a certain depth upon which sudden deepening without bending occurs, usually without fibrous fracture appearance, and then a reversion takes place to much bending with notch opening until complete separation is reached. The transition point is the initial occurrence of this deepening without concurrent appreciable additional

*In studies of Charpy behavior above and below the transition temperature, the writer has sectioned Charpy bars perpendicularly to the notch after various amounts of permanent bending and observed the notch behavior in the text. A good reference is "Notched Bar Impact Testing" a discussion arranged by the Manchester Association of Engineers, reprinted in the Transactions of the Association, Volume 1937-1938.

bending. It coincides with incipient falling off in energy absorption as temperature is lowered. The deepening without appreciable bending increases as temperature is lowered. The energy absorption is relatively small when the section is no longer in the completely yielded state.

Specification of an upper limit to the Charpy transition temperature, depending on yield strength, has been extensively used to avoid brittle failure in, for example, gun barrels where, without this specification, failure occurs with so little evidence of ductility that fragments of the barrel may often be fitted together into the original shape. No regard seems to be paid to the fact that at this limit there is energy absorption with much bending preceding the fracture, but fracture appearance is noted and emphasized even to the extent that the first disappearance, as test temperature is lowered, of complete fibrosity is sometimes taken to be the point of transition. Very frequently, the energy transition can be seen to occur at the same point. The apparent discrepancy in ductility between the barrel failure and the Charpy test failure may be more important than real, however, since the transition (with sudden deepening and concomitant energy drop) referred to above occurs approximately at the center of the section where the straining is presumably small. Indeed, for some materials and applications, the transition temperature is taken to be the temperature where the energy absorption is some fraction (usually one half) of that where the energy absorption first falls off (and the sudden deepening begins) as test temperature is lowered. This, of course, may possibly approximate the result of the present analysis.

The procedure for treating this Charpy-type transition does not differ basically from that explored here for K_{Ic} test conditions of small-scale yielding. The same stress-strain curve fracture model may be used but, of course, the stress formulae are more complicated than their limiting near the notch tip form.

In Parts I, II, and III, all stresses σ must be replaced by $\sigma/(k/2)$ if the stress concentration coefficient $k \neq 2$ in the elastic formula for stress at the tip of the crack-like (i.e., $a/\rho \gg 1$) notch being treated:

$$\sigma = p k \sqrt{a/\rho}.$$

The notation k is also given by the ratio of analytical expressions for K , i.e.,

$$\frac{k}{2} = \frac{K \text{ for notch being treated}}{K \text{ for central notch in a wide plate}}$$

The k and K expressions are for loading forces perpendicular to the crack axis, so-called Mode I.

PART I. TRANSITION TEMPERATURE AND ASSOCIATED PROPERTIES SIMPLY BASED ON NOTCH ELASTIC STRESS

Normal and Shearing Stresses along Crack Axis

We assume the stresses are the same as those usually computed from elasticity theory for crack-like notches, see Appendix A.

Let $r/a = x/a = u^2/2$ be the coordinate along the crack axis, positive away from the crack opening, into the material. The "a" is an important reference dimension, usually a crack depth or half crack length, as in the case of a central crack in a wide plate, which we shall assume in what follows. The tip is located at $x/a = (\rho_0/a)/2$ where $\rho = \rho_0$ is the tip radius. Besides being a measure of distance, u is also the parameter of parabolic coordinates, one of which may be assumed to be coincident with the notch, and $u = \sqrt{\rho/a}$, where ρ is the tip radius of any of these parabolae. See Appendix A for details.

The loading stress $p(=S_1)$ acts perpendicularly to the crack axis. Since this notch is assumed to be very narrow and deep relatively to the tip radius, i.e., to be "crack-like," and since we suppose the difference between p and the loading stress (if any) along the crack axis to be much less than the yield strength of the material, the latter loading stress does not appear in the expression for stresses near the notch tip.

We assume plane strain such that the difference of principal normal stresses is $2Y/\sqrt{3}$ where Y is the usual tensile yield strength of the material.

The maximum shearing stress, one half of the difference of the principal normal stresses, along the crack axis is

$$S_s = \frac{u_{00}^2}{u^3} p$$

where u_{00} is the effective value of $\sqrt{\rho/a}$ at the notch tip.

Thus, yielding occurs from u_{00} to u where

$$u^3 = \frac{u_{00}^2}{Y/\sqrt{3}} p$$

i.e., to the yield limit

$$u = \left(\frac{u_{00}^2}{Y/\sqrt{3}} p \right)^{1/3} \equiv u_Y.$$

The normal stress acting perpendicularly to the crack axis (principal stress) is

$$S = \left[\left(\frac{u_{00}}{u} \right)^2 + 1 \right] \frac{p}{u}.$$

Thus, S at the yield limit is

$$S = \frac{Y}{\sqrt{3}} \left[1 + \left(\frac{p\sqrt{3}}{Y u_{00}} \right)^{2/3} \right]$$

or

$$S = \frac{Y}{\sqrt{3}} \left[1 + \left(\frac{\sqrt{3}}{L_{00}} \right)^{2/3} \right]$$

with

$$L_{00} \equiv \frac{Y u_{00}}{p} = \frac{Y \sqrt{\rho_{00}}}{p \sqrt{a}} = \frac{Y \sqrt{\rho_{00}}}{K}$$

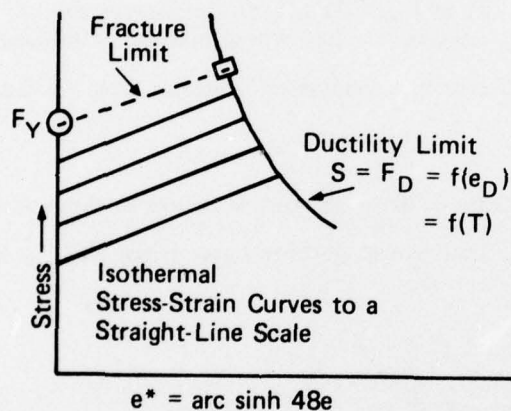
where $K = p\sqrt{a}$ is a fracture mechanics parameter of toughness.

S at the notch tip, $u = u_{00}$ is simply

$$\begin{aligned}
 S &= \left[\left(\frac{u_{00}}{u_{00}} \right)^2 + 1 \right] \frac{p}{u_{00}} \\
 &= \frac{2p}{u_{00}} \\
 &= 2p \sqrt{\frac{a}{\rho_{00}}} \\
 &= \frac{2K}{\sqrt{\rho_{00}}}.
 \end{aligned}$$

Fracture and Transition Temperatures

1. Fracture in General



We shall assume fracture or failure occurs in accordance with the accompanying stress-strain fracture diagram,* as discussed below. The stress strain curves are those for constant temperature and strain rate, the lower the temperature and the higher the strain rate, the higher the curve. The curves are what may be expected for steel.

We presume failure may occur either at the notch tip, or below the notch tip at the yield border, depending on the temperature and strain rate.

For subsurface failure at the yield boundary we have what we call "nil-ductility" fracture corresponding to attainment of the nil-ductility fracture stress F_Y , indicated on the diagram as the starting point of the fracture limit curve. This fracture curve has a shape like that of the stress-strain curves below it, but fracture occurs at the beginning of it for there we first reach a stress sufficient to cause fracture (intermediate points on the curve may be reached, e.g., by prestraining at a higher temperature than corresponds to the fracture curve before loading at the fracture curve temperature).

*This diagram is a particular case of a representation of stress-strain-fracture material behavior that has been much used by what is now known as AMMRC and has been the subject of much investigation by it and under service contracts to it, by Syracuse University. The most extensive report, though it does not cover all work, is Deformation Characteristics of Face Centered Cubic and Hexagonal Metals and Alloys, Project No. AI-9-R-6-04-AW-P3, Contract No. DA-31-124-ARO-D-112 put together cooperatively by AMMRC and Syracuse University and issued by Syracuse University Office of Sponsored Programs, Dept. of Chem. Engr. and Matls. Sci., Syracuse University, N.Y. 13210.

F_Y may also be reached by adding a hydrostatic tension to a lower curve. This may occur subsurface of the notch. (In the tension test the hydrostatic tension is caused by necking. It may also be caused by an artificial neck or a notch.)

However, in contrast, the material at the notch tip is strained in the same way as a flat tension specimen with no possibility of attaining F_Y except by lowering temperature or increasing strain rate. In fact, for some materials the temperature cannot be lowered sufficiently to reach F_Y .

Thus, failure at the notch tip will be on the ductility limit unless the temperature is so low that the notch material is on the fracture stress-strain curve.

Depending on the shape of the stress-strain curves and the position of the ductility limit, one may anticipate that high temperature failure is at the notch tip and low temperature failure is subsurface.

Thus, we have:

$S = F_Y = \text{constant}$, the nil-ductility fracture stress, for subsurface fracture

$S = F_D = \text{variable}$, the ductile fracture stress which varies with the ductility strain and hence with temperature and strain rate.

$F_D = F_{DC} = F_D$ Critical, when $F_Y = 2Y/\sqrt{3}$ on the stress-strain curve, though at initial yielding subsurface F_Y may be reached when, because of hydrostatic tension, $F_Y > 2Y/\sqrt{3}$.

If R.A. is the reduction of area in a plane strain tension test, the ductility strain e_D is given by

$$e_D = \ln \left(\frac{1}{1-R.A.} \right)$$

provided there is no necking which leads to premature failure through addition of a hydrostatic tension.

A stress-strain curve whose limit is the fracture curve when $Y = F_Y$ is

$$S = Y + S_0 \operatorname{arc} \sinh 4.8e$$

or for plain strain

$$S = \frac{2}{\sqrt{3}} \left[Y + S_0 \operatorname{arc} \sinh 4.8e \right]$$

(For most steels $S_0 \cong 15$ ksi, but for some may be 20 or even 30.)

$$Y = Y_0 + C/T$$

using the equation of the envelope of the straight line segments of the actual Y versus T curve. Y_0 , especially, depends on tempering temperature (author's formula).

Hence,

$$F_D = \frac{2}{\sqrt{3}} \left[Y + S_0 \operatorname{arc} \sinh 4.8e_D \right]$$

and we assume that in the region of interest that the ductility limit is given by

$$F_D e_D = F_{D0} e_{D0} = \text{constant}$$

where F_{D0} and e_{D0} are any known corresponding values obtained experimentally.

2. Notch Formulae

At the notch tip

$$S = \frac{2K}{\sqrt{\rho_{00}}}$$

or

$$K = \frac{S\sqrt{\rho_{00}}}{2}$$

which at the ductility limit $S = F_D$ is

$$K = \frac{F_D \sqrt{\rho_{00}}}{2}$$

Subsurface at incipient yielding

$$S_Y = \frac{Y}{\sqrt{3}} \left\{ 1 + \left[\frac{K}{(Y/\sqrt{3})\sqrt{\rho_{00}}} \right]^{2/3} \right\}$$

or

$$K = (Y/\sqrt{3})\sqrt{\rho_{00}} \left[\frac{S_Y}{Y/\sqrt{3}} - 1 \right]^{3/2}$$

3. Transition Yield Strength and Temperature

Fracture occurs at the notch tip if $S = F_D$ and subsurface if $S = S_Y = F_Y$. Although the stress at the notch tip is greater than the subsurface stress and thus $S_{\text{notch tip}} > S_Y$ always, $F_D > F_Y$ so that fracture may not occur first at the tip. If tests at different temperatures are considered, starting at a suitably high temperature, transition will occur from failure at the notch tip to failure subsurface at the transition temperature. Since $K = p\sqrt{a}$ represents the load; whether we consider the stress at one place or the other, the transition is given through

$$K = \frac{F_D \sqrt{\rho_{00}}}{2} = \frac{Y \sqrt{\rho_{00}}}{\sqrt{3}} \left[\frac{F_Y}{Y/\sqrt{3}} - 1 \right]^{3/2}$$

i.e., independent of ρ_{00}

$$\frac{F_D}{2Y/\sqrt{3}} = \left[\frac{F_Y}{Y/\sqrt{3}} - 1 \right]^{3/2}$$

or

$$F_Y = \frac{Y}{\sqrt{3}} \left\{ 1 + \left[\frac{F_D}{2(Y/\sqrt{3})} \right]^{2/3} \right\}$$

Here, since

$$F_D = \frac{2}{\sqrt{3}} \left[Y + S_0 \operatorname{arc} \sinh \frac{48 F_{D0} e_{D0}}{F_D} \right],$$

$$Y = \frac{\sqrt{3}}{2} F_D - S_0 \operatorname{arc} \sinh \frac{48 F_{D0} e_{D0}}{F_D}.$$

Thus, with $F_{D0}e_{D0}$ known in

$$F_D e_D = F_{D0} e_{D0}$$

and C and Y_0 known in

$$T = \frac{C}{Y - Y_0}$$

we may find the mutual transition connection of F_Y , F_D , Y , and T .

Thus, assuming F_D , we compute Y from

$$Y = \frac{\sqrt{3}}{2} F_D - S_0 \operatorname{arc} \sinh \frac{48 F_{D0} e_{D0}}{F_D}$$

then, using this Y , F_Y from

$$F_Y = \frac{Y}{\sqrt{3}} \left\{ 1 + \left[\frac{F_D}{2(Y/\sqrt{3})} \right]^{2/3} \right\}$$

and then T from

$$T = \frac{C}{Y - Y_0}$$

From tables or curves showing these variables, we may select one of interest, for example, $T=T_T$, the transition temperature corresponding to a known F_Y .

Note that raising Y_0 or C raises T_T independently of the other variables. (Y_0 decreases as tempering temperature increases.)

We now consider a few examples of the use of these formulae and the results to be expected, see Tables 1 to 3.

Toughness

It would seem from the foregoing that the toughness K could be computed from

$$K = \frac{F_D \sqrt{\rho_{00}}}{2}$$

above the transition temperature and from

$$K = (Y/\sqrt{3})(\sqrt{\rho_{00}}) \left[F_Y/(Y/\sqrt{3}) - 1 \right]^{3/2}$$

below the transition temperature and from either formula at the transition temperature.

However, the values obtained from these formulae are suspect in terms of our estimates for steel. Consider the transition value. Then if

$$\sqrt{\rho_{00}} \sim 1/30$$

$$F_D \sim 420 \text{ to } 600 \text{ ksi}$$

Table 1. TRANSITION YIELD STRENGTH AND TEMPERATURE VERSUS FRACTURE STRENGTHS FOR NOMINAL WORK HARDENING AND HIGH DUCTILITY (TEMPERING TEMPERATURE $\sim 1/Y_0$).

Work Hard: $S_0 = 15$ ksi; Ductility Limit: $E_{D0}e_{D0} = (160)(3/4) = 120$ ksi;
Activation: $C = 10^4$ °K ksi; Hard Level: $H \sim 2Y_0$.

Y_0 (ksi)	F_D	Y	F_Y	T (°K)	T (°F)
200	320	223.36	277.86	427.94	310.89
	330	232.48	288.25	307.84	94.71
	340	241.59	298.63	240.43	-26.62
	350	250.69	309.00	197.29	-104.27
150	270	177.52	225.65	363.41	194.74
	280	186.72	236.12	272.31	30.76
	290	195.91	246.59	217.83	-67.31
	300	205.08	257.03	181.57	-132.58
250	380	277.90	340.03	358.45	185.80
	390	286.94	350.35	270.66	27.78
	400	295.99	360.67	217.46	-67.98

Note: the linear and almost equal variation of Y and F_Y corresponding to the linear variation of F_D as well as the large variation in T.
Note: °F = (1.8) (°K) - 459.4
 F_D and F_Y may be found by linear interpolation of the above for any T (e.g., T = 32°F) with Y from $Y = Y_0 + C/T$.

Table 3. TRANSITION YIELD STRENGTH AND TEMPERATURE VERSUS FRACTURE STRENGTHS FOR NOMINAL WORK HARDENING AND LOW DUCTILITY (TEMPERING TEMPERATURE $\sim 1/Y_0$).

$S_0 = 15$ ksi; $E_{D0}e_{D0} = 60$ ksi; $C = 10^4$ °K ksi

Y_0 (ksi)	F_D	Y	F_Y	T (°K)	T (°F)
200	310	224.59	275.72	406.63	272.53
	320	233.73	286.11	296.50	74.31
	330	242.85	296.49	233.40	-39.28
	340	251.95	306.86	192.49	-112.91
150	260	178.67	223.51	348.85	168.52
	270	187.89	233.99	263.92	15.66
	280	197.09	244.44	212.35	-77.18
	290	206.28	254.89	177.69	-139.55
250	370	279.19	337.89	342.58	157.25
	380	288.25	348.21	261.46	11.23
	390	297.29	358.52	211.45	-78.80
	400	306.33	368.83	177.53	-139.85

Table 2. TRANSITION YIELD STRENGTH AND TEMPERATURE VERSUS FRACTURE STRENGTHS FOR ZERO AND HIGH WORK HARDENING (TEMPERING TEMPERATURE $\sim 1/Y_0$).

$S_0 = 0$; $C = 10^4$ °K ksi

Y_0 (ksi)	F_D	Y	F_Y	T (°K)	T (°F)
200	260	225.17	260	397.35	255.84
	270	233.83	270	295.62	72.72
	280	242.49	280	235.37	-35.74
	290	251.15	290	195.51	-107.47
150	380	226.71	298.70	374.44	214.58
	390	236.14	309.41	276.67	38.60
	400	245.56	320.10	219.48	-64.34
	410	254.96	330.77	181.94	-131.90
100	330	179.18	244.67	342.69	157.43
	340	188.74	255.55	258.16	5.29
	350	198.26	266.37	207.19	-86.45
	360	207.77	277.14	173.11	-147.81
50	430	273.71	352.06	421.81	299.86
	440	283.06	362.67	302.52	85.14
	450	292.39	373.26	235.92	-34.75
	460	301.71	383.84	193.40	-111.27

Note: For $S_0 = 0$, and $T^\circ K = 273$, $T^\circ F = 32$, $10^4/273 + Y_0 = 36.63 + Y_0 = Y$ and $F_D = (2\sqrt{3})Y$.
Hence if $Y_0 = 250$, $Y = 286.63$; if $Y_0 = 200$, $Y = 236.63$; if $Y_0 = 150$, $Y = 186.63$.
Perhaps it is most interesting to say that $Y_0 = Y - 36.63$.

$S_0 = 30$ ksi; $F_{D0}e_{D0} = (160)(3/4) = 120$ ksi; $C = 10^4$ °K ksi

Table 4. TABLE OF $u_0/u_{00} = \sqrt{\rho/\rho_{00}}$ AT THE TRANSITION

$$u_0 = u_{00} \exp \frac{\sqrt{3}}{2} \frac{Y}{E} \exp \left[\frac{M\bar{Y}}{2} \left(\frac{F_D}{Y} - 1 \right) \right]$$

$$\text{where } \bar{Y} = \frac{2Y}{\sqrt{3}}$$

$$\text{i.e., } \sqrt{\frac{\rho}{\rho_{00}}} = \frac{u_0}{u_{00}} = \exp \left[\frac{M\bar{Y}}{2} \left(\frac{F_D}{Y} - 1 \right) \right]$$

F_D/\bar{Y}	$\bar{Y} = 50$ ksi	100	150	200	250	300	
1.5	1.133	1.284	1.455	1.649	1.868	2.117	$E_{tan} = 150$ ksi $M = 10^{-2}$
2	1.284	1.649	2.117	2.718	3.490	4.48	
2.5	1.455	2.117	3.080	4.482	6.521	9.488	
3	1.649	2.718	4.482	7.389	12.182	20.086	
1.5	1.084	1.133	1.206	1.284	1.367	1.455	$E_{tan} = 300$ ksi $M = 1/2 \times 10^{-2}$
2	1.133	1.284	1.455	1.649	1.868	2.117	
2.5	1.206	1.455	1.755	2.117	2.554	3.080	
3	1.284	1.649	2.117	2.718	3.490	4.481	
1.5	1.043	1.087	1.133	1.181	1.232	1.284	$E_{tan} = 450$ ksi $M = 1/3 \times 10^{-2}$
2	1.087	1.181	1.284	1.396	1.517	1.649	
2.5	1.133	1.284	1.455	1.649	1.868	2.117	
3	1.181	1.396	1.649	1.948	2.301	2.718	
1.5	1.032	1.064	1.098	1.133	1.169	1.206	$E_{tan} = 600$ ksi $M = 1/4 \times 10^{-2}$
2	1.064	1.133	1.206	1.284	1.367	1.455	
2.5	1.098	1.206	1.325	1.455	1.598	1.755	
3	1.133	1.284	1.455	1.649	1.868	2.117	

we have

$$K = 420/60 \text{ to } 600/60 \text{ ksi } \sqrt{\text{in.}}$$

$$= 7 \text{ to } 10$$

where we might expect $K \sim 70 \text{ ksi } \sqrt{\text{in.}}$. (We are not questioning the use of the above formulae for transition calculations by the above consideration, because the exact formulae have a mutual dependency which may make them insensitive to alterations in form as the notch is loaded.)

Thus, we consider the use of a formula for stress, which is based on incremental considerations. That is, the stress is the sum of stress increments based on the instantaneous notch geometry corresponding to the load as it is built up. At the notch tip it is approximately, assuming yielding at the tip has occurred,

$$S \cong \frac{4E_t}{3} \ln((u_0/u_{00}) + 2Y/\sqrt{3})$$

$$\cong \frac{4E_t}{3} \ln \frac{(3/2)(p/E_t) - u_{00} \left[(\sqrt{3}Y)/(2E_t) - 1 \right]}{u_{00}} + 2Y/\sqrt{3}$$

$$\cong \frac{4E_t}{3} \ln \left\{ (3/2) [p/(E_t u_{00})] - (\sqrt{3} Y)/(2E_t) + 1 \right\} + 2Y/\sqrt{3}$$

where u_0 is the value of u at the notch tip when the loading is p , as shown by the second and third formulae. Then $u_0 = u_{00}$ when $p = 0$. E_t is the modulus of the stress-strain curve beyond the yield point; we assume here that it is suitably represented by the secant modulus drawn from the yield point. Thus since

$$S = \frac{2}{\sqrt{3}} [Y + S_0 \text{ arc sinh } 48e]$$

and we are concerned with the modulus to F_D , e_D ,

$$E_t \cong \frac{F_D - 2Y/\sqrt{3}}{e_D} = \frac{2}{\sqrt{3}} \frac{S_0}{e_D} \text{ arc sinh } 48e_D$$

or

$$= 48 (F_D - 2Y/\sqrt{3}) / \sinh \left[(F_D - 2Y/\sqrt{3}) / (2S_0/\sqrt{3}) \right].$$

Now let us examine our formula for S , where $S = F_D$

$$F_D = \frac{4E_t}{3} \ln \left\{ (3/2) [p/(E_t u_{00})] - (\sqrt{3} Y)/(2E_t) + 1 \right\} + 2Y/\sqrt{3}.$$

If p is small so that the $\{ \}$ term is ~ 1 ,

$$F_D \rightarrow \frac{4E_t}{3} \left\{ (3/2) [p/(E_t u_{00})] - (\sqrt{3} Y)/(2E_t) \right\} + 2Y/\sqrt{3} = 2p/u_{00}$$

our usual formula for stress at the base of the notch, and our former expression from which we found K , since $u_{00} = \sqrt{\rho_{00}/a}$ and $K = p\sqrt{a}$.

Substituting $K = p\sqrt{a}$, our formula for F_D becomes

$$F_D = \frac{4E_t}{3} \ln \left\{ \frac{3}{2} \frac{K}{E_t \sqrt{\rho_{00}}} - \frac{\sqrt{3}}{2} \frac{Y}{E_t} + 1 \right\} + \frac{2Y}{\sqrt{3}}$$

so that

$$\frac{K}{\sqrt{\rho_{00}}} = \frac{Y}{\sqrt{3}} + \frac{2E_t}{3} \left\{ \exp \frac{F_D - \sqrt{3}Y}{4E_t/3} - 1 \right\}.$$

We may also express this formula for $K/\sqrt{\rho_{00}}$ in terms of S_0 , F_D , and Y alone or S_0 , e_D , and Y alone by insertion of our secant formulae for E_t , i.e.,

$$\frac{K}{\sqrt{\rho_{00}}} = \frac{Y}{\sqrt{3}} + (32) \frac{F_D - 2Y\sqrt{3}}{\sinh\left(\frac{F_D - 2Y\sqrt{3}}{2S_0\sqrt{3}}\right)} \left\{ \exp \frac{\sinh[(F_D - 2Y\sqrt{3})/(2S_0/E_t)]}{64} - 1 \right\}$$

and

$$\frac{K}{\sqrt{\rho_{00}}} = \frac{Y}{\sqrt{3}} + \frac{4}{3} \frac{S_0/e_D}{\sqrt{3}} \operatorname{arc} \sinh 48e_D \left\{ \exp \frac{3e_D}{4} - 1 \right\}.$$

In the last expression, note the heavy dependence of K on Y and S_0 .

Thus, if

$$Y = 200 \text{ ksi}$$

$$F_D - 2Y\sqrt{3} = 100 \text{ ksi}$$

$$S_0 = 15 \text{ ksi}$$

$$\frac{K}{\sqrt{\rho_{00}}} = 361.026$$

by the first of these two formulae, so that if $\sqrt{\rho_{00}} = 1/30$, $K = 12.034$.

Suppose,

$$e_D = \ln 20 \cong 3$$

$$Y = 200 \text{ ksi}$$

$$S_0 = 15 \text{ ksi}.$$

Then,

$$\frac{K}{\sqrt{\rho_{00}}} = 300.475$$

by the second of these two expressions so that if $\sqrt{\rho_{00}} = 1/30$, $K = 10.016$. If $e_D = 4$, $K/\sqrt{\rho_{00}} = 552.606$ and if $\sqrt{\rho_{00}} = 1/30$, $K = 18.420 \text{ ksi}\sqrt{\text{in.}}$. If S_0 were 45, $K/\sqrt{\rho_{00}} = 1426.878$ and with $\sqrt{\rho_{00}}$ again equal to $1/30$, $K = 47.563$. In this $K = 142.688$.

Note on Tip Radius

In the above treatment u_0 was closely expressed by

$$\frac{u_0}{u_{00}} = \frac{3}{2} \frac{p}{E_t u_{00}} - \frac{\sqrt{3} Y}{2 E_t} + 1$$

where $u_0 = \sqrt{\rho_0/a}$, $u_{00} = \sqrt{\rho_{00}/a}$. Since $K = p\sqrt{a}$ this may be written

$$\frac{\sqrt{\rho_0}}{\sqrt{\rho_{00}}} = \frac{3}{2E_t} \left[\frac{K}{\sqrt{\rho_{00}}} - \frac{Y}{\sqrt{3}} \right] + 1$$

which on substituting our expression for E_t becomes

$$\frac{\sqrt{\rho_0}}{\sqrt{\rho_{00}}} = \frac{3\sqrt{3}}{4} \left[\frac{e_D/S_0}{\text{arc sinh } 48e_D} \right] \left[\frac{K}{\sqrt{\rho_{00}}} - \frac{Y}{\sqrt{3}} \right] + 1.$$

Examples:

Let $e_D = 3$, $S_0 = 15$ ksi, $Y = 200$ ksi.

Then

$$\frac{\sqrt{\rho_0}}{\sqrt{\rho_{00}}} = 0.045878 \left[\frac{K}{\sqrt{\rho_{00}}} - 115.47 \right] + 1.$$

If $K = 10$ and $\sqrt{\rho_{00}} = 1/30$,

$$\sqrt{\rho_0} = 0.3155.$$

If $K = 50$ and $\sqrt{\rho_{00}} = 1/30$,

$$\sqrt{\rho_0} = 2.1507.$$

If $K = 10$ and $\sqrt{\rho_{00}} = 1/10$,

case is impossible; notch has not yielded.

If $K = 50$ and $\sqrt{\rho_{00}} = 1/10$,

$$\sqrt{\rho_0} = 1.8642.$$

These figures indicate that the tip becomes quite blunt as failure is approached. If the blunted region is very small, this may not be observed by crack opening displacement measurements. In particular, if we artificially flatten the tip of a narrow parabolic notch under load, the opening of the sides near the tip would give no indication of the real tip configuration, although the measurements of such opening might very well be used to compute a radius which may be effective for some analyses. Such, for example, may be the determination of the significant portion, for strength considerations, of the slip line structure.

In the absence of explicit experimental proof of the existence of radii such as we have computed, one may choose to believe that the tip radius discussed here will be found to be connected to an actual radius to be computed without making the simplification that the stresses are the same as those of linear elasticity theory. In any case, the radius drops out in the determination of transition yield strength and temperature.

PART II. TRANSITION PROPERTIES CONFORMING TO A TWO-SEGMENT STRESS-STRAIN CURVE AND ASSOCIATED FINITE BOUNDARY DISPLACEMENTS

We assume the stresses are from usual elasticity theory for crack-like notches, but that the strains are from a two-straight-line stress-strain relationship and that boundary movements and other deformations may be large.

Strains in Parabolic Coordinates

$$x/a = (u^2 - v^2)/2 \text{ and } y/a = u v$$

where u and v are the parabolic coordinates.

$$\frac{\partial(x/a)}{\partial u} = u \qquad \frac{\partial(y/a)}{\partial u} = v$$

$$\frac{\partial(x/a)}{\partial v} = -v \qquad \frac{\partial(y/a)}{\partial v} = u$$

$$h_u^2 = h_v^2 = (u^2 + v^2) \equiv h^2.$$

It is well to remember that on the $v = 0$ (crack) axis, that $u = \sqrt{2x/a}$ is not only a measure of distance to a parabola tip, but $u = \sqrt{\rho/a}$ also, where ρ is the tip radius of the parabola. In particular, $u_0 = \sqrt{\rho_0/a}$ where ρ_0 is the tip radius of the bounding parabola.

Let U and V be the displacements in the u and v directions.

Then,

$$\begin{aligned} e_u &= \frac{1}{h} \left(\frac{\partial U}{\partial u} + \frac{V}{h} \frac{\partial h}{\partial v} \right) \\ &= \frac{1}{h} \left(\frac{\partial U}{\partial u} + \frac{vV}{h^2} \right) \\ e_v &= \frac{1}{h} \left(\frac{\partial V}{\partial v} + \frac{U}{h} \frac{\partial h}{\partial u} \right) \\ &= \frac{1}{h} \left(\frac{\partial V}{\partial v} + \frac{uU}{h^2} \right) \\ \gamma_{uv} &= \frac{\partial}{\partial v} \left(\frac{U}{h} \right) + \frac{\partial}{\partial u} \left(\frac{V}{h} \right) \\ &= \frac{1}{h} \left(\frac{\partial U}{\partial v} + \frac{\partial V}{\partial u} \right) - \frac{1}{h^2} \left(U \frac{\partial h}{\partial v} + V \frac{\partial h}{\partial u} \right). \end{aligned}$$

Thus, on the crack axis where $v = V = 0$,

$$e_u = \frac{1}{u} \frac{\partial U}{\partial u}.$$

Near Tip Elastic Stresses in Parabolic Coordinates

$$h^4 \sigma_u/p = -u_0^2 u + u^3$$

$$h^4 \sigma_v/p = -u_0^2 u + u(u^2 + 2v^2)$$

$$h^4 \sigma_{uv}/p = -u_0^2 v + v u^2$$

where

$$h^2 = u^2 + v^2.$$

Thus, on the crack axis, $v = 0$,

$$\sigma_u = \left[1 - \left(\frac{u_0}{u} \right)^2 \right] \frac{p}{u}$$

$$\sigma_v = \left[1 + \left(\frac{u_0}{u} \right)^2 \right] \frac{p}{u}$$

$$\sigma_{uv} = 0$$

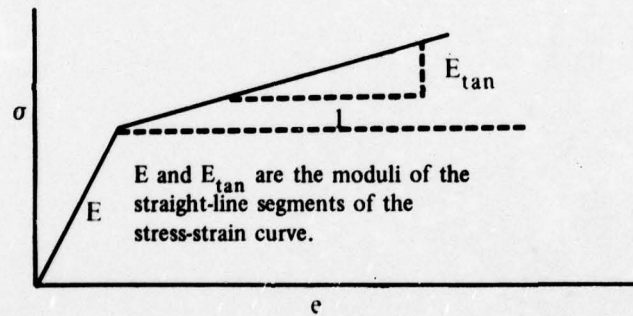
and

$$\sigma_v + \sigma_u = \frac{2p}{u}$$

$$\sigma_v - \sigma_u = 2 \left(\frac{u_0}{u} \right)^2 \frac{p}{u}.$$

Strain for Plane Strain with a Piecewise Linear Stress Strain Relation

(Ref: J. W. Hutchinson, Eq. 35, J. Mech. Phys. Solids, v. 16, 1968)



$$\sigma_e = \text{equivalent tensile stress, } \sigma_e^2 = 3/2 S_{ij} S_{ij}$$

$$S_{ij} = \sigma_{ij} - (1/3) \sigma_{kk} \delta_{ij}$$

$$\lambda = (3/2) (E/E_{tan} - 1) \text{ if } \sigma_\theta/Y > 1$$

$$\lambda = 0 \text{ if } \sigma_\theta/Y \leq 1$$

$$a = (1 - Y/\sigma_e).$$

The stress-strain curve is (Hutchinson)

$$Ee_{ij} = (1 + \nu)\sigma_{ij} - \nu \sigma_{pp} \delta_{ij} + \lambda (1 - Y/\sigma_e) S_{ij}$$

thus for plane strain

$$Ee_{11} = (1+\nu)\sigma_{11} - \nu(\sigma_{11} + \sigma_{22} + \sigma_{33}) + \lambda a \left(\sigma_{11} - \frac{\sigma_{11} + \sigma_{22} + \sigma_{33}}{3} \right)$$

$$Ee_{22} = (1+\nu)\sigma_{22} - \nu(\sigma_{11} + \sigma_{22} + \sigma_{33}) + \lambda a \left(\sigma_{22} - \frac{\sigma_{11} + \sigma_{22} + \sigma_{33}}{3} \right)$$

$$0 = Ee_{33} = (1+\nu)\sigma_{33} - \nu(\sigma_{11} + \sigma_{22} + \sigma_{33}) + \lambda a \left(\sigma_{33} - \frac{\sigma_{11} + \sigma_{22} + \sigma_{33}}{3} \right).$$

From the expression for e_{33} we have,

$$\begin{aligned} \sigma_{33} &= \frac{\nu + \lambda a/3}{1 + 2\lambda a/3} (\sigma_{11} + \sigma_{22}) \\ &= \beta(\sigma_{11} + \sigma_{22}) \end{aligned}$$

where

$$\beta \equiv \frac{\nu + \lambda a/3}{1 + 2\lambda a/3} \quad \left\{ \begin{array}{l} \text{Note: If } \nu = 1/2, \beta = 1/2. \end{array} \right.$$

Thus introducing* this expression for σ_{33} into the expressions for e_{11} and e_{22} , we have,

$$Ee_{11} = (1 - \beta^2)(1 + 2\lambda a/3) \left[\sigma_{11} - \frac{\beta}{1 - \beta} \sigma_{22} \right]$$

$$Ee_{22} = (1 - \beta^2)(1 + 2\lambda a/3) \left[\sigma_{22} - \frac{\beta}{1 - \beta} \sigma_{11} \right].$$

*For example.

$$\begin{aligned} Ee_{11} &= \sigma_{11} - \nu(\sigma_{22} + \sigma_{33}) + \frac{2\lambda a}{3} \sigma_{11} - \frac{\lambda a}{3}(\sigma_{22} + \sigma_{33}) \\ &= \sigma_{11} (1 + 2\lambda a/3) - (\nu + \frac{\lambda a}{3}) (\sigma_{22} + \sigma_{33}) \\ &= \sigma_{11} (1 + 2\lambda a/3) - \beta(1 + 2\lambda a/3) [\sigma_{22} + (\sigma_{11} + \sigma_{22})\beta] \\ &= (1 + 2\lambda a/3) [\sigma_{11}(1 - \beta^2) - \beta(1 + \beta) \sigma_{22}] \\ &= (1 - \beta^2) (1 + 2\lambda a/3) \left[\sigma_{11} - \frac{\beta}{1 - \beta} \sigma_{22} \right]. \end{aligned}$$

Also, for plane strain,*

$$\sigma_e^2 = (1 - \beta + \beta^2) (\sigma_{22} - \sigma_{11})^2 + (1 - 4\beta + 4\beta^2) \sigma_{22} \sigma_{11} + 3\sigma_{12}^2.$$

Thus, for plane strain, if $\nu = 1/2$

$$\beta = \nu = 1/2$$

$$\sigma_e^2 = (3/4) (\sigma_{22} - \sigma_{11})^2 + 3\sigma_{12}^2$$

[and $\sigma_e = (\sqrt{3}/2) (\sigma_{22} - \sigma_{11})$ where $\sigma_{12} = 0$]

$$\frac{4Ee_{11}}{3} = (\sigma_{11} - \sigma_{22}) (1 + 2\lambda a/3)$$

$$\frac{4Ee_{22}}{3} = (\sigma_{22} - \sigma_{11}) (1 + 2\lambda a/3)$$

where

$$a = 1 - Y/\sigma_e.$$

If $\nu = 0.28$ and $\lambda = 100$, which we assume to be reasonable values,

$$\beta = \frac{0.28 + 100 a/3}{1 + 200 a/3}$$

so that if $a = 1 - Y/\sigma_e = 1 - 1/2 = 1/2$,

$$\beta \geq 0.494$$

and if $a = 1 - 0.9 = 0.1$,

$$\beta \geq 0.471.$$

Thus, for $\lambda \neq 0$, it is especially interesting to make the simplification $\beta = 1/2$ which makes $\nu = \beta = 1/2$.

Strain and Axial Displacement U in Parabolic Coordinates on $v = 0$ Axis, for $\nu = \beta = 1/2$ for a Piecewise Linear Stress-Strain Relation

Setting $e_{11} = e_u$, and $\sigma_{11} = \sigma_u$, $\sigma_{22} = \sigma_v$,

$$\frac{4Ee_u}{3} = (\sigma_u - \sigma_v) (1 + 2\lambda a/3)$$

*For example,

$$\begin{aligned} \sigma_e^2 &= (3/2) S_{ij}; S_{ij} \text{ is also given for plane strain by} \\ 2\sigma_e^2 &= (\sigma_{11} - \sigma_{22})^2 + (\sigma_{11} - \sigma_{33})^2 + (\sigma_{22} - \sigma_{33})^2 + 6\sigma_{12}^2 \\ &= (\sigma_{11} - \sigma_{22})^2 + [\sigma_{11} - \beta(\sigma_{11} + \sigma_{22})]^2 + [\sigma_{22} - \beta(\sigma_{11} + \sigma_{22})]^2 + \sigma_{12}^2 \\ &= (2 - 2\beta + 2\beta^2) (\sigma_{11}^2 + \sigma_{12}^2) - 4\beta(1 - \beta)\sigma_{11}\sigma_{22} - 2\sigma_{11}\sigma_{22} + 6\sigma_{12}^2 \\ &= 2(1 - \beta + \beta^2) (\sigma_{11} - \sigma_{22})^2 + 4(1 - \beta + \beta^2)\sigma_{11}\sigma_{22} - 4\beta(1 - \beta)\sigma_{11}\sigma_{22} - 2\sigma_{11}\sigma_{22} + 6\sigma_{12}^2 \\ &= 2 \left\{ (1 - \beta + \beta^2) (\sigma_{11} - \sigma_{22})^2 + (1 - 4\beta + 4\beta^2) \sigma_{11}\sigma_{22} + 6\sigma_{12}^2 \right\} \end{aligned}$$

with $a = 1 - Y/\sigma_e$

$$= 1 - \frac{Y}{(\sqrt{3}/2)(\sigma_v - \sigma_u)}$$

Thus,

$$e_u = \frac{\sigma_u - \sigma_v}{2}(M) + \frac{\lambda Y}{\sqrt{3}E}$$

← $\frac{M}{\text{Defined}}$

with $M \equiv (3/2 + \lambda)/E$.

We recall that

$$\sigma_v - \sigma_u = 2\left(\frac{u_0}{u}\right)^2 \frac{p}{u}$$

Thus, since (with p constant)

$$e_u = \frac{1}{u} \frac{\partial U}{\partial u}$$

$$U = \int e_u u du = \int \left[-\left(\frac{u_0}{u}\right)^2 Mp + \frac{\lambda Y}{\sqrt{3}E} u \right] du$$

$$= + \frac{u_0^2}{u} Mp + \frac{\lambda Y}{\sqrt{3}E} \frac{u^2}{2} + \text{Const.}$$

Hence, if $\lambda = 0$

$$U = \frac{3}{2} \frac{u_0^2}{u} \frac{p}{E}$$

At the yield point at $u = u_0$, $p = p_Y$

$$\sigma_v - \sigma_u = \frac{2Y}{\sqrt{3}} = \frac{2p_Y}{u_0}$$

Hence U at $u = u_0$, $p = p_Y$ is

$$U_Y = \frac{3}{2} u_0 \frac{p_Y}{E} = \frac{\sqrt{3}}{2} u_0^2 \frac{Y}{E}$$

If $\lambda \neq 0$

$$U = \frac{u_0^2}{u} Mp + \frac{\lambda Y}{\sqrt{3}E} \frac{u^2}{2} + \text{Const}$$

where the constant is determined by equating this expression at $u = u_0$, $p = p_Y = \frac{Y u_0}{\sqrt{3}}$, to U at yield at $u = u_0$ of the $\lambda = 0$ case, i.e.,

$$\frac{\sqrt{3}}{2} u_0^2 \frac{Y}{E} = u_0 M \left(\frac{Y u_0}{\sqrt{3}} \right) + \frac{\lambda Y}{\sqrt{3}E} \frac{u_0^2}{2} + \text{Const.}$$

Therefore, if $\lambda = 0$,

$$U = \frac{u_0^2}{u} Mp + \frac{\lambda Y}{2\sqrt{3}E} (u^2 - 3u_0^2) \quad p \geq p_Y.$$

However, determination of the constant was unnecessary to the case where we are concerned only with a change in U caused by a change in p .

In fact, this expression is not the same as an expression for U that takes account of the change in u as loading proceeds.

INCREMENTAL THEORY

Relation between Instantaneous and Initial Values of u for $v = 0$

Let $x \equiv u_0/u$ and U refer to the previously derived equation for U based on stationary u .

Then,

$$\begin{aligned} du &= \frac{U \text{ at } p + dp - U \text{ at } p}{h} \\ &= x^2 M dp \end{aligned}$$

since $h = u$ for $v = 0$ and $M \equiv (3/2 + \lambda)/E$.

Thus,

$$du_0 = M dp$$

and

$$\begin{aligned} dx &= d(u_0/u) = (u du_0 - u_0 du)/u^2 \\ &= \frac{x}{u_0} (du_0 - x du) \\ &= x (1 - x^3) M \frac{dp}{u_0} \\ &= x (1 - x^3) \frac{du_0}{u_0} \end{aligned}$$

i.e.,

$$du = x^2 M dp$$

$$du_0 = M dp$$

$$dx = [x(1 - x^3)M dp]/u_0.$$

← dx versus dp/u₀

By elimination of dp from du and du_0 it is readily seen that

$$u^3 - u_0^3 = \text{Const.}$$

Thus, if

$$u_i - \text{initial value of } u$$

and

u_{00} = initial value of u_0

we see that

$$u^3 - u_1^3 = u_0^3 - u_{00}^3$$

independent of the value of λ .

u_0 versus p :

Since

$$du_0 = M dp,$$

$$u_0 = Mp + \text{Const.}$$

If $\lambda = 0$

$$u_0 - u_{00} = (3/2) (p/E)$$

since u_{00} is the initial value of u_0 and M is $(3/2)/E$ when $\lambda = 0$.

At yield

$$u_{0Y} - u_{00} = (3/2) (p_Y/E)$$

If $\lambda = 0$

$$u_0 = Mp + \text{Const.}$$

$$u_{0Y} = M p_Y + \text{Const.}$$

i.e.,

$$u_0 - u_{0Y} = M(p - p_Y).$$

Stresses

In our previous nonincremental theory, we replace p by dp and the stresses by differential stresses so that we have only an incremental stress, corresponding to an incremental pressure, when the coordinates have the instantaneous values u , including $u = u_0$, or x , i.e.,

$$d\sigma_u = x (1 - x^2) (dp/u_0)$$

$$d\sigma_v = x (1 + x^2) (dp/u_0)$$

$$\sigma_{uv} = 0$$

$$d\bar{S} \equiv d(\sigma_v + \sigma_u) = 2x (dp/u_0)$$

$$d\bar{D} \equiv d(\sigma_v - \sigma_u) = 2x^3 (dp/u_0).$$

We recall that,

$$du = x^2 M dp$$

$$du_0 = M dp$$

and

\leftarrow u versus u_1

$$\frac{dx}{x(1-x^3)} = M (dp/u_0)$$

and note that there is a one to one relationship between p and u at any specified location, in particular between p and u_0 , the coordinate of the notch tip.

For \bar{D} we have, from

$$du = x^2 M dp$$

and

$$d\bar{D} = 2x^3 (dp/u_0) = 2x^2 (dp/u),$$

$$d\bar{D} = (2/M) (du/u)$$

$$\bar{D} = (2/M) \ln u + \text{Const.}$$

Thus, for $\lambda = 0$, since $D = 0$ when $u = u_i$

$$\bar{D} = (4E/3) \ln (u/u_i)$$

where $u^3 = u_0^3 + u_i^3 - u_{00}^3$ in terms of the initial coordinate of the place where \bar{D} is desired and the notch tip coordinate u_0 which represents the load, i.e.,

$$u_0 - u_{00} = (3/2) (p/E).$$

At the yield point, at the base of the notch, whether or not $\lambda = 0$, we have $u = u_0 = u_{0Y}$ so that

$$\bar{D} = \bar{S} = \frac{2Y}{\sqrt{3}} = \frac{4E}{3} \ln \frac{u_{0Y}}{u_{00}}$$

i.e.,

$$u_{0Y} = u_{00} \exp\left(\frac{\sqrt{3} Y}{2 E}\right)$$

$$\cong u_{00} \left(1 + \frac{\sqrt{3} Y}{2 E}\right)$$

and,

$$\frac{p_Y}{E} = \frac{2u_{00}}{3} \left[\exp\left(\frac{\sqrt{3} Y}{2 E}\right) - 1 \right].$$

If $\lambda \neq 0$

$$\bar{D} = \frac{2}{M} \ln \frac{u}{u_{0Y}} + \frac{2Y}{\sqrt{3}}$$

$$= \frac{2}{3M} \ln \frac{u_i^3 + u_0^3 - u_{00}^3}{u_{0Y}^3} + \frac{2Y}{\sqrt{3}}$$

and

$$p = p_Y + (1/M) (u_0 - u_{0Y}).$$

We note that if $u = u_0$ and $\lambda \neq 0$

$$\bar{D} = \bar{S} = \frac{2}{M} \ln \frac{u_0}{u} + \frac{2Y}{\sqrt{3}}$$

For \bar{S} we have,

$$\begin{aligned} d\bar{S} &= 2x \frac{dp}{u_0} \\ &= \frac{2x}{M} \times \frac{dx}{(1-x^3)} \\ &= \frac{2}{M} \frac{dx}{1-x^3} \end{aligned}$$

Thus

$$\begin{aligned} \bar{S} &= \frac{2}{M} \left\{ \frac{1}{6} \ln \frac{1-x^3}{(1-x)^3} + \frac{1}{\sqrt{3}} \tan^{-1} \frac{2x+1}{\sqrt{3}} \right\} + \text{Const.} \\ &= \frac{2}{M} \left\{ \frac{1}{6} \ln \frac{u^3 - u_0^3}{(u - u_0)^3} + \frac{1}{\sqrt{3}} \tan^{-1} \frac{2u_0/u + 1}{\sqrt{3}} \right\} + \text{Const.} \end{aligned}$$

For $\lambda = 0$, \bar{S} is zero when $u_0 = u_{00}$, $u = u_i$. Hence,

$$\begin{aligned} \bar{S} &= \frac{4E}{3} \left\{ \frac{1}{6} \ln \frac{(u^3 - u_0^3)}{(u - u_0)^3} \frac{(u_i - u_{00})^3}{(u_i^3 - u_{00}^3)} + \frac{1}{\sqrt{3}} \tan^{-1} \frac{2u_0/u + 1}{\sqrt{3}} - \frac{1}{\sqrt{3}} \tan^{-1} \frac{2u_{00}/u_i + 1}{\sqrt{3}} \right\} \\ &= \frac{4E}{3} \left\{ \frac{1}{2} \ln \frac{u_i - u_{00}}{u - u_0} + \frac{1}{\sqrt{3}} \tan^{-1} \frac{2u_0/u + 1}{\sqrt{3}} - \frac{1}{\sqrt{3}} \tan^{-1} \frac{2u_{00}/u_i + 1}{\sqrt{3}} \right\} \end{aligned}$$

since, again $u^3 - u_0^3 = u_i^3 - u_{00}^3$.

Since

$$\frac{u_i - u_{00}}{u - u_0} = \frac{u_i^3 - u_{00}^3}{u^3 - u_0^3} \cdot \frac{u^2 + uu_0 + u_0^2}{u_i^2 + u_i u_{00} + u_{00}^2}$$

\bar{S} may also be written

$$\bar{S} = \frac{4E}{3} \left\{ \frac{1}{2} \ln \frac{u^2 + u u_0 + u_0^2}{u_i^2 + u_i u_{00} + u_{00}^2} + \frac{1}{\sqrt{3}} \tan^{-1} \frac{2u_0/u + 1}{\sqrt{3}} - \frac{1}{\sqrt{3}} \tan^{-1} \frac{2u_{00}/u_i + 1}{\sqrt{3}} \right\}$$

which expression has the advantage that it may be more readily interpreted as $u_i \rightarrow u_{00}$, $u \rightarrow u_0$.

If $u_i = u_{00}$, $u = u_0$

$$\begin{aligned} \bar{S}_{u = u_0} &= \bar{S}_{u_i = u_{00}} = (4E/3) \{ \ln (u_0/u_{00}) \} \\ &u_i = u_{00} \end{aligned}$$

in agreement with our former result for \bar{D} .

For $\lambda \neq 0$, we note that \bar{S} may also be written as follows.

$$\begin{aligned}\bar{S} &= \frac{2}{M} \left\{ \frac{1}{6} \ln \frac{(u^3 - u_0^3)(u^2 + u u_0 + u_0^2)}{(u^3 - u_0^3)^3} + \frac{1}{\sqrt{3}} \tan^{-1} \frac{2u_0/u + 1}{\sqrt{3}} \right\} + \text{Const.} \\ &= \frac{2}{M} \left\{ \frac{1}{2} \ln (u^2 + u u_0 + u_0^2) - \frac{1}{3} \ln (u^3 - u_0^3) + \frac{1}{\sqrt{3}} \tan^{-1} \frac{2u_0/u + 1}{\sqrt{3}} \right\} + \text{Const.} \\ &= \frac{2}{M} \left\{ \frac{1}{2} \ln (u^2 + u u_0 + u_0^2) - \frac{1}{3} \ln (u^3 - u_0^3) + \frac{1}{\sqrt{3}} \tan^{-1} \frac{2u_0/u + 1}{\sqrt{3}} \right\} + \text{Const.}\end{aligned}$$

When $u = u_0 = u_{0Y}$, $\bar{S} = 2Y/\sqrt{3}$. Therefore

$$2Y/\sqrt{3} = (2/M) \left\{ (1/2) \ln (3u_{0Y}^2) - (1/3) \ln (u_{0Y}^3 - u_{0Y}^3) + (1/\sqrt{3}) \tan^{-1} \sqrt{3} \right\} + \text{Const.}$$

from which we have the expression for the constant.

Thus,

$$\bar{S} = \frac{2}{M} \left\{ \frac{1}{2} \ln \frac{u^2 + u u_0 + u_0^2}{3u_{0Y}^2} + \frac{1}{\sqrt{3}} \tan^{-1} \frac{2u_0/u + 1}{\sqrt{3}} - \frac{1}{\sqrt{3}} \tan^{-1} \sqrt{3} \right\} + \frac{2Y}{\sqrt{3}}.$$

We note that if $u = u_0$ this expression becomes

$$\bar{S} = (2/M) \ln (u_0/u_{0Y}) + 2Y/\sqrt{3}$$

as obtained in the analysis for \bar{D} . It also satisfies the differential equation from which it was derived if account is taken that $d(u^3 - u_0^3) = 0$.

Since

$$\begin{aligned}\tan^{-1} \frac{2u_0/u + 1}{\sqrt{3}} - \tan^{-1} \sqrt{3} &= \tan^{-1} \tan \left[\tan^{-1} \frac{2u_0/u + 1}{\sqrt{3}} \tan^{-1} \sqrt{3} \right] \\ &= \tan^{-1} \frac{\frac{2u_0/u + 1}{\sqrt{3}} - \sqrt{3}}{1 + \left(\frac{2u_0/u + 1}{\sqrt{3}} \right) \sqrt{3}} \\ &= \tan^{-1} \frac{1}{\sqrt{3}} \frac{u_0 - u}{u_0 + u}\end{aligned}$$

\bar{S} may also be written ($\lambda \neq 0$)

$$\bar{S} = \frac{2}{M} \left\{ \frac{1}{2} \ln \frac{u^2 + u u_0 + u_0^2}{3u_{0Y}^2} + \frac{1}{\sqrt{3}} \tan^{-1} \frac{(u_0 - u)}{\sqrt{3}(u_0 + u)} \right\} + \frac{2Y}{\sqrt{3}}.$$

Since

$$\bar{S} = \sigma_v + \sigma_u$$

$$\bar{D} = \sigma_v - \sigma_u$$

we have

$$\sigma_v = (\bar{S} + \bar{D})/2$$

$$\sigma_u = (\bar{S} - \bar{D})/2.$$

Thus, for $\lambda = 0$

$$2\sigma_v = \frac{4E}{3} \left\{ \frac{1}{2} \ln \frac{u^2 + uu_0 + u_0^2}{u_i^2 + u_i u_{00} + u_{00}^2} + \frac{1}{\sqrt{3}} \tan^{-1} \frac{2u_0/u + 1}{\sqrt{3}} - \frac{1}{\sqrt{3}} \tan^{-1} \frac{2u_{00}/u_i + 1}{\sqrt{3}} \right\} + \frac{4E}{3} \ln \frac{u}{u_i}$$

i.e.,

$$\sigma_v = \frac{2E}{3} \left\{ \frac{1}{2} \ln \left[\frac{u^2 (u^2 + uu_0 + u_0^2)}{u_i^2 (u_i^2 + u_i u_{00} + u_{00}^2)} \right] + \frac{1}{\sqrt{3}} \left[\tan^{-1} \frac{2u_0/u + 1}{\sqrt{3}} - \tan^{-1} \frac{2u_{00}/u_i + 1}{\sqrt{3}} \right] \right\}$$

$$\sigma_u = \frac{2E}{3} \left\{ \frac{1}{2} \ln \left[\frac{u_i^2 (u^2 + uu_0 + u_0^2)}{u^2 (u_i^2 + u_i u_{00} + u_{00}^2)} \right] + \frac{1}{\sqrt{3}} \left[\tan^{-1} \frac{2u_0/u + 1}{\sqrt{3}} - \tan^{-1} \frac{2u_{00}/u_i + 1}{\sqrt{3}} \right] \right\}$$

$\lambda \neq 0$

$$2\sigma_v = \frac{2}{M} \left\{ \frac{1}{2} \ln \frac{u^2 + uu_0 + u_0^2}{3u_0Y^2} + \frac{1}{\sqrt{3}} \tan^{-1} \frac{(u_0 - u)}{\sqrt{3}(u_0 + u)} \right\} + \frac{2Y}{\sqrt{3}} + \frac{2}{M} \left\{ \frac{1}{2} \ln \frac{u^2}{u_0Y^2} \right\} + \frac{2Y}{\sqrt{3}}$$

$$\sigma_v = \frac{1}{M} \left\{ \frac{1}{2} \ln \left[\frac{u^2 (u^2 + uu_0 + u_0^2)}{3u_0Y^4} \right] + \frac{1}{\sqrt{3}} \tan^{-1} \frac{(u_0 - u)}{\sqrt{3}(u_0 + u)} \right\} + \frac{2Y}{\sqrt{3}}$$

$$\sigma_u = \frac{1}{M} \left\{ \frac{1}{2} \ln \left[\frac{u^2 + uu_0 + u_0^2}{3u^2} \right] + \frac{1}{\sqrt{3}} \tan^{-1} \frac{(u_0 - u)}{\sqrt{3}(u_0 + u)} \right\}$$

Transition

By transition we mean a change in failure location from notch tip surface to a position below the surface. It is presumed that the subsurface failure is more brittle and cataclysmic.

In this analysis we use a maximum stress failure criterion where the stress necessary for failure depends on the amount of plastic straining. The fracture stress at the surface is F_D , occurring with ductility (subscript D) since the material at the tip is under simple (plane strain) tension, while the subsurface fracture stress is F_Y occurring with very little ductility (subscript Y signifying proximity to initial yielding) since it takes place at or close to the elastic-plastic boundary under a combined-stress condition involving considerable hydrostatic tension. Although the yield strength Y is on the same stress-strain curve as F_D , F_Y is greater than Y at the transition so that the hydrostatic tension is necessary to reach it. And while the stress distribution below the notch tip is such that the maximum stress at any location there is always less than that at the tip, F_Y is less than F_D so that both F_D and F_Y may be reached simultaneously. This is the condition for the transition. It is a relationship between F_D , F_Y and Y. The temperature dependence of the transition is dependent on that of F_D and Y, especially the latter.

We consider the case in which $\lambda \neq 0$ because we are interested in the maximum stress σ_v at the elastic-plastic boundary.

Since

$$\bar{D} = \frac{2}{M} \ln \frac{u}{u_{0Y}} + \frac{2Y}{\sqrt{3}},$$

we have

$$\frac{u}{u_{0Y}} = 1 \text{ for } \bar{D} = \frac{2Y}{\sqrt{3}},$$

the elastic-plastic boundary.

$$\sigma_v = \frac{1}{M} \left\{ \frac{1}{2} \ln \left[\frac{u^2 (u^2 + uu_0 + u_0^2)}{3u_{0Y}^4} \right] + \frac{1}{\sqrt{3}} \tan^{-1} \frac{(u_0 - u)}{\sqrt{3}(u_0 + u)} \right\} + \frac{2Y}{\sqrt{3}}$$

Thus at $u/u_{0Y} = 1$,

$$\sigma_v \text{ at } u/u_{0Y} = 1 = \frac{1}{M} \left\{ \frac{1}{2} \ln \frac{1 + \frac{u_0}{u_{0Y}} + \left(\frac{u_0}{u_{0Y}}\right)^2}{3} + \frac{1}{\sqrt{3}} \tan^{-1} \frac{\left(\frac{u_0}{u_{0Y}} - 1\right)}{\sqrt{3}\left(\frac{u_0}{u_{0Y}} + 1\right)} \right\} + \frac{2Y}{\sqrt{3}}$$

whereas at the base of the notch, $u = u_0$,

$$\begin{aligned} \sigma_v \text{ base of notch} &= \frac{1}{M} \left\{ \frac{1}{2} \ln \left(\frac{u_0}{u_{0Y}}\right)^4 + 0 \right\} + \frac{2Y}{\sqrt{3}} \\ &= \frac{2}{M} \ln \frac{u_0}{u_{0Y}} + \frac{2Y}{\sqrt{3}}. \end{aligned}$$

Thus, the transition takes place when σ_v at $u/u_{0Y} = 1$ is F_Y and σ_v at the base of the notch is F_D , i.e.,

$$F_Y = \frac{1}{M} \left\{ \frac{1}{2} \ln \frac{1 + R + R^2}{3} + \frac{1}{\sqrt{3}} \tan^{-1} \frac{R - 1}{\sqrt{3}(R + 1)} \right\} + \frac{2Y}{\sqrt{3}}$$

$$F_D = \frac{2}{M} \ln R + \frac{2Y}{\sqrt{3}}$$

where $R \equiv u_0/u_{0Y}$.

Since

$$R = \exp \left[\frac{M}{2} \left(F_D - \frac{2Y}{\sqrt{3}} \right) \right], \quad M \equiv \frac{3/2 + \lambda}{E}$$

F_Y for transition is readily found from known F_D and Y by solving for R and substituting this value into the expression for F_Y .

Note that the crack tip radius does not appear in this expression for transition. The introduction of fracture stress F_D absorbs the radius. To some extent one may regard the tip radius as a mathematical parameter computed from F_D , loading stress, and crack depth, rather than an actual or effective or average tip radius.

Transition: Approximation

Here we compare the above formula with the simple formula for transition which does not take into account the change in boundary associated with loading. We do this by showing that each reduces to the same approximate form.

We consider the above formula under the assumption that the exponent of the expression for R is small, i.e.,

$$R - 1 \cong \frac{M}{2} \left(F_D - \frac{2Y}{\sqrt{3}} \right).$$

(This might not be true for a very flat stress-strain curve, i.e., if $\lambda = (3/2) (E/E_{\tan} - 1)$ is very large.)

Exactly,

$$F_Y = \frac{1}{M} \left\{ \frac{1}{2} \ln \frac{1 + (1 + \overline{R-1}) + (1 + \overline{R-1})^2}{3} + \frac{1}{\sqrt{3}} \tan^{-1} \frac{R-1}{\sqrt{3}(2 + R-1)} \right\} + \frac{2Y}{\sqrt{3}}$$

which, if $\overline{R-1}$ is small, becomes

$$\begin{aligned} F_Y &\cong \frac{1}{M} \left\{ \frac{1}{2} \ln(1 + \overline{R-1}) + \frac{1}{\sqrt{3}} \tan^{-1} \frac{\overline{R-1}}{2\sqrt{3}} \right\} + \frac{2Y}{\sqrt{3}} \\ &\cong \frac{1}{M} \left\{ \frac{\overline{R-1}}{2} + \frac{\overline{R-1}}{6} \right\} + \frac{2Y}{\sqrt{3}} \\ &= \frac{2}{3M} (R-1) + \frac{2Y}{\sqrt{3}} \\ &= \frac{2}{3M} \left[\frac{M}{2} \left(F_D - \frac{2Y}{\sqrt{3}} \right) \right] + \frac{2Y}{\sqrt{3}} \end{aligned}$$

i.e.,

$$F_Y \cong \frac{1}{3} \left(F_D - \frac{2Y}{\sqrt{3}} \right) + \frac{2Y}{\sqrt{3}}$$

i.e., F_Y is equal to the yield strength in plane strain plus one third of the difference between F_D and this yield strength.

Our simple theory, which did not include changes in the boundary under load, led to the formula

$$F_D = \frac{2Y}{\sqrt{3}} \left[\frac{F_Y}{Y\sqrt{3}} - 1 \right]^{3/2}$$

We make our approximation to this by considering the case in which

$$\frac{(F_Y - 2Y/\sqrt{3})}{Y\sqrt{3}} \ll 1.$$

That is, exactly,

$$F_D = \frac{2Y}{\sqrt{3}} \left[\frac{(F_Y - 2Y\sqrt{3}) + 2Y\sqrt{3}}{Y\sqrt{3}} - 1 \right]^{3/2}$$

$$= \frac{2Y}{\sqrt{3}} \left[1 + \frac{F_Y - 2Y\sqrt{3}}{Y\sqrt{3}} \right]^{3/2}$$

becomes, on the above approximation,

$$F_D \cong \frac{2Y}{\sqrt{3}} \left[1 + \frac{3}{2} \frac{F_Y - 2Y\sqrt{3}}{Y\sqrt{3}} \right]$$

i.e.,

$$F_Y \cong \frac{1}{3} \left(F_D - \frac{2Y}{\sqrt{3}} \right) + \frac{2Y}{\sqrt{3}}$$

as before.

Loading Stress and Toughness at the Transition

We recollect that (p19)

$$p = p_Y + \frac{1}{M} (u_0 - u_{0Y})$$

i.e.,

$$p = p_Y + \frac{u_{0Y}}{M} (R - 1)$$

where

$$R \equiv u_0/u_{0Y} = \exp \left[\frac{M}{2} (F_D - 2Y\sqrt{3}) \right]$$

$$u_{0Y} = u_{00} \exp \left(\frac{\sqrt{3}}{2} \frac{Y}{E} \right)$$

$$p_Y = \frac{2E}{3} (u_{0Y} - u_{00}) = \frac{2Eu_{00}}{3} \left[\exp \frac{\sqrt{3}}{2} \frac{Y}{E} - 1 \right]$$

$$u_{00} = \sqrt{p_{00}/a}.$$

Hence, the loading stress is

$$p = u_{00} \left\{ \frac{\exp \left(\frac{\sqrt{3}}{2} \frac{Y}{E} \right) - 1}{(3/2)E} + \frac{\exp \left(\frac{\sqrt{3}}{2} \frac{Y}{E} \right)}{M} \left[\exp \left[\frac{M}{2} (F_D - 2Y\sqrt{3}) \right] - 1 \right] \right\}$$

and the toughness $K = p\sqrt{a}$ is

$$K = \sqrt{\rho_{00}} \left\{ \frac{\exp\left(\frac{\sqrt{3} Y}{2 E}\right) - 1}{(3/2)/E} + \frac{\exp\left(\frac{\sqrt{3} Y}{2 E}\right)}{M} \left[\exp\left[\frac{M}{2} (F_D - 2Y/\sqrt{3})\right] - 1 \right] \right\}$$

at the transition.

Approximately,

$$\frac{K}{\sqrt{a}} = p \cong \frac{\sqrt{\rho_{00}}}{\sqrt{a}} \left\{ \frac{Y}{\sqrt{3}} + \frac{\exp\left[\frac{M}{2} (F_D - 2Y/\sqrt{3})\right] - 1}{M} \right\}$$

or, if the second portion of the stress-strain curve is not too flat (i.e., M too large),

$$\frac{K}{\sqrt{a}} = p = \frac{F_D}{2} \sqrt{\frac{\rho_{00}}{a}}$$

at the transition.

We append Table 4 of $\sqrt{\rho/\rho_{00}}$ at the transition to convey an idea of how much ρ may differ from ρ_{00} and of the value of the exponential term in the above formula. Although we believe that $E_{\tan} = 300$ ksi is probably most representative for steel, it may be less and if this is the case, it may be seen (according to this model) that the tip radius ρ under load at the transition may be far greater than its no-load value. Likewise, in this case, according to the above formula, K will be significantly increased over the value it would have if the second portion of the stress-strain curve were steeper.

PART III. TRANSITION PROPERTIES BASED ON NOTION OF ELASTICALLY LIMITED STRAIN AND A SLIP LINE THEORY

We assume that the strains are from usual elasticity theory for crack-like notches on the argument that even in the yielded region they are substantially contained within a fairly rigid elastic mass.

Contained Strain Theory and Comparison with the Contained Stress Theories

In a paper called "Characteristics of Crack Failure"¹ Beeuwkes presented a curve which he used to determine subsurface fracture stress and crack tip radius from experimental curves of G_{Ic} or K_{Ic} versus yield strength \bar{Y} which, in turn, is a function of test temperature or tempering temperature. The curve may also be considered to be the transition relationship between F_Y , F_D , and \bar{Y} , for a change in fracture location from notch tip surface to subsurface, or vice versa, as \bar{Y} is changed, as will be explained below. We take $\bar{Y} = 2\bar{Y}/\sqrt{3}$, the plane strain yield strength.

The basis of the curve is the determination of the subsurface stress F_Y through the hydrostatic addition of stress associated with the change in direction of the shear stress trajectory having the greatest change in crossing the yielded region. The flow strength in the vicinity of this trajectory was found to be very near the yield strength \bar{Y} . A parabolically shaped tip was assumed so that the stress increased with load, i.e., yielding; with no tip radius all trajectories are the same and consequently there is no increase in stress with yielding. The subsurface hydrostatic stress at the yield boundary is solely due to the change in direction of a trajectory and the yield strength, not with work hardening.

The abscissae of the curve are the angular changes in direction corresponding to the different degrees of yielding. In these F_Y is connected by the relationship $\bar{Y} + \bar{Y} \alpha = F_Y$, i.e., $\alpha = F_Y/\bar{Y} - 1$ assuming the fracture prolongs the crack.*

*Fracture along a line perpendicular to the crack axis may occur under the stress $\bar{Y} \alpha$ if the fracture stress across this direction is sufficiently low.

The ordinates are values of

$$L \equiv \frac{\bar{Y}}{p} \sqrt{\frac{\rho}{a}}$$

which may be written

$$\begin{aligned} L &\equiv \frac{\bar{Y}/\bar{E}}{[p\sqrt{a\rho}/\bar{E}]} \\ &= \frac{\bar{Y}/\bar{E}}{e_D/2} = \frac{\bar{Y}/E}{K/(E\sqrt{\rho})} \end{aligned}$$

where \bar{E} is the Young's modulus for plane strain,

$$\bar{E} \equiv E/(1 - \nu^2)$$

$$K = p\sqrt{a} = \text{toughness}$$

$2p\sqrt{a/\rho}$ = virtual stress at the notch tip, i.e., stress by elastic formula

$(2p\sqrt{a/\rho})/\bar{E} = e_D$ = actual strain at the notch tip assuming contained strain.

Although this strain is computed elastically, it is valid beyond the yield point on the assumption that the case is one of small-scale yielding largely surrounded by a fairly rigid though elastic region. Thus $e_D = F_D/\bar{E}_s$ is the ductility strain if fracture separation occurs at the tip. Here, \bar{E}_s is the secant modulus corresponding to a line drawn on the tensile stress-strain diagram of the material used, from the origin to the fracture point where the actual stress is $\sigma = F_D$.

Thus, also

$$L = \frac{2Y}{(\bar{E}/\bar{E}_s)F_D}$$

Hence, letting f stand for "function of," the curve may be written

$$L = f(\sphericalangle)$$

i.e.,

$$L \text{ or } \frac{\bar{Y}/\bar{E}}{K/(E\sqrt{\rho})} \text{ or } \frac{\bar{Y}/E}{e_D/2} \text{ or } \frac{2 E_s/E}{F_D/Y} = f\left(\frac{F_Y}{Y} - 1\right)$$

since $\bar{E}_s = F_D/e_D$ by definition and $\bar{E}_s/\bar{E} = E_s/E$.

Thus, we have expressed the curve L versus \sphericalangle in terms of variables associated with our model of transition which is that this point occurs at a yield strength with which ductile fracture at the tip occurs simultaneously with essentially brittle subsurface fracture. That this L versus \sphericalangle curve is the transition relationship follows from the assumption that the relationship of these variables is for practicable purposes unique. Simultaneous fracture means that at some yield strength the load p required to reach F_D or e_D is the same as that required to reach F_Y . Thus, p and the cross-axis stress σ_y at the yield boundary (on the crack axis) are uniquely related to each other for fixed \bar{Y} , as are p/\bar{Y} and σ_y/\bar{Y} . Likewise, p and the strain e at the notch tip are uniquely related to each other for a given material with its stress-strain curve, as are p/\bar{Y} and e/e_Y where $e_Y = \bar{Y}/E$, the yield strain. Hence, whatever the stress-strain curve, the condition that e/e_Y is reached at the same load as σ_y/\bar{Y} , is found

by elimination of p/\bar{Y} from the $p/\bar{Y} = f(\sigma_v/\bar{Y})$ and $p/\bar{Y} = f(e/e_Y)$ relations. The e is the e_D corresponding to $\sigma_v = F_D$ for the stress-strain curve with its specific value of \bar{Y} . If \bar{Y} is the only parameter specifying a set of stress-strain curves (i.e., one to each value of \bar{Y}), e_D and F_D may be found for each \bar{Y} and the group of these form the transition relationship for the specific type of stress-strain curve under consideration.

We now make the assumption for this application, that for practical purposes \bar{Y} sufficiently characterizes the usual engineering stress-strain curves, for we have seen that F_Y is practically only determined by \bar{Y} from the standpoint of effect of materials properties, in our derivation of the L versus α curve, and by hypothesis the notch tip reaches e_D, F_D . Both F_D and F_Y are postulated from prior knowledge of the material and are therefore reached at the transition. It appears, therefore, that the effect of shape of the stress-strain curve would only be to affect the place where F_Y occurs and with this the amount of angular change of direction of the shear stress trajectories. This is unlikely to be very significant since, again, they undergo their change in direction in a region where the flow stress is practically equal to the yield strength \bar{Y} .

In analyses of the K_{Ic} versus Y curves of steel versus test temperature or tempering temperature $1 + \alpha = \frac{F_Y}{\bar{Y}} = 2$ to 2.50. In this range the L versus α curve may be approximated by

$$\begin{aligned} L &\approx 0.95 [1 - 0.56 \alpha] \\ &= 0.95 [1 - 0.56 (F_Y/\bar{Y} - 1)] \\ &= 0.532 [2.768 - F_Y/\bar{Y}]. \end{aligned}$$

From this, if $F_Y/\bar{Y} = 2$, $L = 0.418$, and if $F_Y/\bar{Y} = 2.5$, $L = 0.152$.

Such analyses also indicate that (at the load corresponding to K_{Ic} measurement)

$$\sqrt{\rho} \sim 1/30 \sqrt{\text{in.}}$$

From the above, in general, in the range $2 \leq 1 + \alpha \leq 2.5$,

$$L \text{ or } \frac{\bar{Y}/\bar{E}}{K/(\bar{E}\sqrt{\rho})} \text{ or } \frac{\bar{Y}/\bar{E}}{e_D/2} \text{ or } \frac{2 E_s/E}{F_D/\bar{Y}} = 0.532 \left[2.786 - \frac{F_Y}{\bar{Y}} \right].$$

We note especially that toughness

$$K = (\bar{E} e_D \sqrt{\rho})/2$$

so long as the failure is not subsurface, i.e., so long as we are "above" the transition.

Let us suppose that valid K_{Ic} measurements really do correspond to the transition, and see how well, if at all, values for L and K derived with the aid of the above expressions coincide with our expectations from experience.

Case A

Let $F_Y/\bar{Y} = 2$, hence $L = 0.418$

Assume $\sqrt{\rho} = 1/30$

Reasonable expectations:

$\bar{Y} = 280$ ksi

$\bar{E} = 28,000$ ksi

$e_D = 0.20$

$K = 25$ ksi $\sqrt{\text{in.}}$

$L = \frac{\bar{Y}/\bar{E}}{e_D/2} = 0.10$

$K = (\bar{E} e_D \sqrt{\rho})/2 = 93$

Case B

$F_Y/\bar{Y} = 2.5$, hence $L = 0.152$

Assume $\sqrt{\rho} = 1/30$

Reasonable expectations:

$\bar{Y} = 200$ ksi

$\bar{E} = 28,000$ ksi

$e_D = 0.40$

$K = 50$ ksi $\sqrt{\text{in.}}$

$L = 0.035$

$K = 186$

A comparison between the calculated and postulated values of L and K shows that had the computations been made with values of e_D one quarter as great as the expected tension test values used, the values of L and K would have closely agreed with those postulated. However, agreement would also be reached with retention of the values of e_D , by using a notch stress concentration factor four times as large as the one employed, i.e., $8\sqrt{a/\rho}$ instead of $2\sqrt{a/\rho}$ on the speculative basis that the actual irregular notch front is four times as severe a stress concentrator as the smooth tip assumed. By this argument the 2's on the left side of the transition formulae above are replaced by 8's.

APPENDIX A. Near Tip Stresses along a Crack-Like Notch Axis in Terms of Polar, Rectangular, and Parabolic Coordinates for a Loading Stress Acting Perpendicularly to the Notch Axis.

The expression for the stresses in terms of polar coordinates (r, θ) is the same as that in rectangular coordinates taking the crack axis to be $\theta = 0$.

The equivalent loading stress acting far from the notch and perpendicularly to it is S_1 . The loading stress along the axis S_{1x} does not appear in the expressions for near tip stresses for crack-like notches ($a/\rho \gg 1$). k_1 is the stress concentration coefficient, i.e., $S = k_1 S_1 \sqrt{a/\rho}$ at the notch tip for such notches; $k_1 = 2$ for the elliptical crack in the center of a wide plate which is loaded perpendicularly to the crack axis.

In the following expressions, the tip of the notch is at a distance $\rho/2$ from the origin of coordinates, which is within the notch.

Polar and Rectangular Coordinates

$$\frac{2 S_\theta}{k_1 S_1} = \frac{\rho/a}{(2r/a)^{3/2}} + \frac{1}{(2r/a)^{1/2}}$$

$$\frac{2 (S_\theta - S_r)}{k_1 S_1} = \frac{2\rho/a}{(2r/a)^{3/2}}$$

Here ρ is the radius of the notch tip.

Parabolic Coordinates

In parabolic coordinates (u, v) where $v = 0$ when $\theta = 0$ and $r/a (=x/a) = u^2/2$ and the tip radius is given by $u = \sqrt{\rho/a}$ for any of the coordinate parabolas with their differing values of ρ , including that of the notch itself

$$\frac{2 S_v}{k_1 S_1} = \frac{\rho/a}{u^3} + \frac{1}{u}$$

$$\frac{2 (S_v - S_u)}{k_1 S_1} = \frac{2\rho/a}{u^3}$$

where S_v acts perpendicularly to the crack axis and S_u along the crack axis. In these expressions ρ is the radius of the notch tip itself.

In the body of the report a notation for tip radius is taken over from the writer's analyses taking account of load-induced change in tip radius. Thus, the radius of the tip of the crack in the unloaded condition is ρ_0 with $u_0 = \sqrt{\rho_0/a}$ and in the loaded condition ρ with $u_0 = \sqrt{\rho_0/a}$.

DISTRIBUTION LIST

No. of Copies		No. of Copies	To
1	Office of the Director, Defense Research and Engineering, The Pentagon, Washington, D.C. 20301		Commander, U. S. Army Foreign Science and Technology Center, 220 7th Street, N. E., Charlottesville, Virginia 22901
12	Commander, Defense Documentation Center, Cameron Station, Building 5, 5010 Duke Street, Alexandria, Virginia 22314	1	ATTN: Mr. Marley, Military Tech
1	Metals and Ceramics Information Center, Battelle Columbus Laboratories, 505 King Avenue, Columbus, Ohio 43201		Chief, Benet Weapons Laboratory, LCWSL, USA ARBADC, Watervliet Arsenal, Watervliet, New York 12189
1	Deputy Chief of Staff, Research, Development, and Acquisition, Headquarters Department of the Army, Washington, D. C. 20310	1	ATTN: DRDAR-LCB-TL
1	ATTN: DAMA-ARZ		Director, Eustis Directorate, U. S. Army Air Mobility Research and Development Laboratory, Fort Eustis, Virginia 23604
1	Commander, Army Research Office, P. O. Box 12211, Research Triangle Park, North Carolina 27709	1	ATTN: Mr. J. Robinson, DAVDL-E-MOS (AVRADCOM)
1	ATTN: Information Processing Office		U. S. Army Aviation Training Library, Fort Rucker, Alabama 36360
1	Dr. F. W. Schmiedeshoff	1	ATTN: Building 5906-5907
1	Commander, U. S. Army Materiel Development and Readiness Command, 5001 Eisenhower Avenue, Alexandria, Virginia 22333		Commander, U. S. Army Agency for Aviation Safety, Fort Rucker, Alabama 36362
1	ATTN: DRCLDC, Mr. R. Zentner	1	ATTN: Librarian, Bldg. 4905
1	Commander, U. S. Army Communications Research and Development Command, Fort Monmouth, New Jersey 07703		Commander, USACDC Air Defense Agency, Fort Bliss, Texas 79916
1	ATTN: DRCCO-GG-TD	1	ATTN: Technical Library
1	DRCCO-GG-DM		Commander, U. S. Army Engineer School, Fort Belvoir, Virginia 22060
1	Commander, U. S. Army Missile Research and Development Command, Redstone Arsenal, Alabama 35809	1	ATTN: Library
1	ATTN: DRDMI-RKK, Mr. C. Martens, Bldg. 7120		Commander, U. S. Army Engineer Waterways Experiment Station, Vicksburg, Mississippi 39180
1	Commander, U. S. Army Natick Research and Development Command, Natick, Massachusetts 01760	1	ATTN: Research Center Library
1	ATTN: Technical Library		Commander, U. S. Army Mobility Equipment Research and Development Center, Fort Belvoir, Virginia 22060
1	Dr. E. W. Ross	1	ATTN: DRDME-MW, Dr. J. W. Bond
1	DRDNA-UE, Dr. L. A. McClaine		Commander, Naval Air Engineering Center, Lakehurst, New Jersey 08733
1	Commander, U. S. Army Satellite Communications Agency, Fort Monmouth, New Jersey 07703	1	ATTN: Technical Library, Code 1115
1	ATTN: Technical Document Center		Director, Structural Mechanics Research, Office of Naval Research, 800 North Quincy Street, Arlington, Virginia 22203
1	Commander, U. S. Army Tank-Automotive Research and Development Command, Warren, Michigan 48090	1	ATTN: Dr. N. Perrone
1	ATTN: DRDTA-RKA		Naval Air Development Center, Aero Materials Department, Warminster, Pennsylvania 18974
1	DRDTA-UL, Technical Library	1	ATTN: J. Viglione
2	Commander, U. S. Army Armament Research and Development Command, Dover, New Jersey 07801		David Taylor Naval Ship Research and Development Laboratory, Annapolis, Maryland 21402
1	ATTN: Technical Library	1	ATTN: Dr. H. P. Chu
1	DRDAR-SCM, J. D. Corrie		Naval Research Laboratory, Washington, D.C. 20375
1	Dr. J. Fraiser	1	ATTN: C. D. Beachem, Head, Adv. Mat'l's Tech Br. (Code 6310)
1	Commander, White Sands Missile Range, New Mexico 88002	1	Dr. J. M. Krafft - Code 8430
1	ATTN: STEWS-WS-VT	1	E. A. Lange
1	Commander, Aberdeen Proving Ground, Maryland 21005	1	Dr. P. P. Puzak
1	ATTN: STEAP-TL, Bldg. 305	1	R. J. Sanford - Code 8436
1	Commander, U. S. Army Armament Research and Development Command, Aberdeen Proving Ground, Maryland 21010	1	A. M. Sullivan
1	ATTN: DRDAR-QAC-E	1	R. W. Rice
1	Commander, U. S. Army Ballistic Research Laboratory, Aberdeen Proving Ground, Maryland 21005	1	S. W. Freiman
1	ATTN: Dr. R. Vitali	1	Dr. Jim C. I. Chang
1	Dr. G. L. Filbey		Chief of Naval Research, Arlington, Virginia 22217
1	Dr. W. Gillich	1	ATTN: Code 471
1	DRDAR-TSB-S (STINFO)		Naval Weapons Laboratory, Washington, D.C. 20390
1	Commander, Harry Diamond Laboratories, 2800 Powder Mill Road, Adelphi, Maryland 20783	1	ATTN: H. W. Romine, Mail Stop 103
1	ATTN: Technical Information Office	1	Ship Research Committee, Maritime Transportation Research Board, National Research Council, 2101 Constitution Avenue, N. W., Washington, D.C. 20418
1	Commander, Picatinny Arsenal, Dover, New Jersey 07801		Air Force Materials Laboratory, Wright-Patterson Air Force Base, Ohio 45433
1	ATTN: Mr. J. Pearson	2	ATTN: AFML (MXE), E. Morrissey
1	G. Randers-Pehrson	1	AFML (LC)
1	Mr. A. Garcia	1	AFML (LLP), D. M. Forney, Jr.
1	SARPA-RT-S	1	AFML (LNC), T. J. Reinhart
1	Commander, Redstone Scientific Information Center, U. S. Army Missile Research and Development Command, Redstone Arsenal, Alabama 35809	1	AFML (MBC), Mr. Stanley Schulman
1	ATTN: DRDMI-TB	1	AFFDL (FB), Dr. J. C. Halpin
1	Commander, Watervliet Arsenal, Watervliet, New York 12189		Air Force Flight Dynamics Laboratory, Wright-Patterson Air Force Base, Ohio 45433
1	ATTN: Dr. T. Davidson	1	ATTN: AFFDL (FBS), C. Wallace
1	Mr. D. P. Kendall	1	AFFDL (FBE), G. D. Sendeckyj
1	Mr. J. F. Throop		

No. of Copies	To
1	National Aeronautics and Space Administration, Washington, D.C. 20546
1	ATTN: Mr. B. G. Achhammer
1	Mr. G. C. Deutsch - Code RW
1	National Aeronautics and Space Administration, Marshall Space Flight Center, Huntsville, Alabama 35812
1	ATTN: R. J. Schwinghamer, EH01, Dir., M&P Lab
1	Mr. W. A. Wilson, EH41, Bldg. 4612
1	National Aeronautics and Space Administration, Langley Research Center, Hampton, Virginia 23665
1	ATTN: Mr. H. F. Hardrath, Mail Stop 188M
1	Mr. R. Foye, Mail Stop 188A
1	National Aeronautics and Space Administration, Lewis Research Center, 21000 Brookpark Road, Cleveland, Ohio 44135
1	ATTN: Mr. S. S. Manson
1	Dr. J. E. Srawley, Mail Stop 105-1
1	Mr. W. F. Brown, Jr.
1	Mr. M. H. Hirschberg, Head, Fatigue Research Section, Mail Stop 49-1
1	National Bureau of Standards, U. S. Department of Commerce, Washington, D.C. 20234
1	ATTN: Mr. J. A. Bennett
1	Mechanical Properties Data Center, Belfour Stulen Inc., 13917 W. Bay Shore Drive, Traverse City, Michigan 49684
1	Mr. W. F. Anderson, Atomics International, Canoga Park, California 91303
1	Midwest Research Institute, 425 Coker Boulevard, Kansas City, Missouri 64110
1	ATTN: Mr. G. Gross
1	Mr. A. Hurlich, Convair Div., General Dynamics Corp., Mail Zone 630-01, P. O. Box 80847, San Diego, California 92138
1	Mr. J. G. Kaufman, Alcoa Research Laboratories, New Kensington, Pennsylvania 15068
1	Mr. P. N. Randall, TRW Systems Group - 0-1/2210, One Space Park, Redondo Beach, California 90278
1	Dr. E. A. Steigerwald, TRW Metals Division, P. O. Box 250, Minerva, Ohio 44657
1	Dr. George R. Irwin, Department of Mechanical Engineering, University of Maryland, College Park, Maryland 20742
1	Mr. W. A. Van der Sluys, Research Center, Babcock and Wilcox, Alliance, Ohio 44601
1	Mr. B. M. Wundt, 2346 Shirl Lane, Schenectady, New York 12309
1	Battelle Columbus Laboratories, 505 King Avenue, Columbus, Ohio 43201
1	ATTN: Mr. J. Campbell
1	Dr. G. T. Hahn
1	R. G. Hoagland, Metal Science Group
1	Dr. E. Rybicki
1	General Electric Company, Schenectady, New York 12010
1	ATTN: Mr. A. J. Brothers, Materials & Processes Laboratory
1	General Electric Company, Schenectady, New York 12309
1	ATTN: Mr. S. Yukawa, Metallurgy Unit
1	Mr. E. E. Zwicky, Jr.
1	General Electric Company, Knolls Atomic Power Laboratory, P. O. Box 1072, Schenectady, New York 12301
1	ATTN: Mr. F. J. Mehringer
1	Dr. L. F. Coffin, Room 1C41-K1, Corp. R&D, General Electric Company, P. O. Box 8, Schenectady, New York 12301
1	United States Steel Corporation, Monroeville, Pennsylvania 15146
1	ATTN: Mr. S. R. Novak
1	Dr. A. K. Shoemaker, Research Laboratory, Mail Stop 78
1	Westinghouse Electric Company, Bettis Atomic Power Laboratory, P. O. Box 109, West Mifflin, Pennsylvania 15122
1	ATTN: Mr. M. L. Parrish
1	Westinghouse Research and Development Center, 1310 Beulah Road, Pittsburgh, Pennsylvania 15235
1	ATTN: Mr. E. T. Wessel
1	Mr. M. J. Manjoine

No. of Copies	To
1	Dr. Alan S. Tetelman, Failure Analysis Associates, Suite 4, 11777 Mississippi Ave., Los Angeles, California 90025
1	Brown University, Providence, Rhode Island 02912
1	ATTN: Prof. J. R. Rice
1	Prof. W. N. Findley, Division of Engineering, Box D
1	Prof. P. C. Paris
1	Carnegie-Mellon University, Department of Mechanical Engineering, Schenley Park, Pittsburgh, Pennsylvania 15213
1	ATTN: Dr. J. L. Swedlow
1	Prof. J. D. Lubahn, Colorado School of Mines, Golden, Colorado 80401
1	Prof. J. Dvorak, Civil Engineering Department, Duke University, Durham, North Carolina 27706
1	George Washington University, School of Engineering and Applied Sciences, Washington, D.C. 20052
1	ATTN: Dr. H. Liebowitz
1	Lehigh University, Bethlehem, Pennsylvania 18015
1	ATTN: Prof. G. C. Sih
1	Prof. R. Roberts
1	Prof. R. P. Wei
1	Prof. F. Erodgan
1	Massachusetts Institute of Technology, Cambridge, Massachusetts 02139
1	ATTN: Prof. B. L. Averbach, Materials Center, 13-5082
1	Prof. F. A. McClintock, Room 1-304
1	Prof. R. M. Pelloux
1	Prof. T. H. H. Pian, Department of Aeronautics and Astronautics
1	Prof. A. S. Argon, Room 1-306
1	Syracuse University, Department of Chemical Engineering and Metallurgy, 409 Link Hall, Syracuse, New York 13210
1	ATTN: Mr. H. W. Liu
1	Dr. V. Weiss, Metallurgical Research Labs., Bldg. D-6
1	Prof. E. R. Parker, Department of Materials Science and Engineering, University of California, Berkeley, California 94700
1	Prof. W. Goldsmith, Department of Mechanical Engineering, University of California, Berkeley, California 94720
1	University of California, Los Alamos Scientific Laboratory, Los Alamos, New Mexico 87544
1	ATTN: Dr. R. Karp
1	Prof. A. J. McEvily, Metallurgy Department U-136, University of Connecticut, Storrs, Connecticut 06268
1	Prof. D. Drucker, Dean of School of Engineering, University of Illinois, Champaign, Illinois 61820
1	University of Illinois, Urbana, Illinois 61801
1	ATTN: Prof. H. T. Corten, Department of Theoretical and Applied Mechanics, 212 Talbot Laboratory
1	Prof. T. J. Dolan, Department of Theoretical and Applied Mechanics
1	Prof. J. Morrow, 321 Talbot Laboratory
1	Mr. G. M. Sinclair, Department of Theoretical and Applied Mechanics
1	Prof. R. I. Stephens, Materials Engineering Division, University of Iowa, Iowa City, Iowa 52242
1	Prof. D. K. Felbeck, Department of Mechanical Engineering, University of Michigan, 2046 East Engineering, Ann Arbor, Michigan 48109
1	Dr. M. L. Williams, Dean of Engineering, 240 Benedum Hall, University of Pittsburgh, Pittsburgh, Pennsylvania 15260
1	Prof. A. Kobayashi, Department of Mechanical Engineering, FU-10, University of Washington, Seattle, Washington 98195
1	State University of New York at Stony Brook, Stony Brook, New York 11790
1	ATTN: Prof. Fu-Pen Chiang, Department of Mechanics
2	Director, Army Materials and Mechanics Research Center, Watertown, Massachusetts 02172
1	ATTN: DRXMR-PL
1	DRXMR-AG-MD
1	Author

